



European Commission

# technical steel research

Measurement and analysis

## Surface inspection of hot bars during rolling



Report

EUR 15814 EN



STEEL RESEARCH



European Commission

# technical steel research

Measurement and analysis

## Surface inspection of hot bars during rolling

D. Savidge

**British Steel, Swinden Technology Centre**  
Moorgate  
Rotherham S60 3AR  
United Kingdom

Contract No 7210-GB/806

1 July 1989 to 30 June 1992

**Final report**

Directorate-General XII  
Science, Research and Development

1996

EUR 15814 EN

## **LEGAL NOTICE**

Neither the European Commission nor any person acting on behalf of the Commission is responsible for the use which might be made of the following information

Cataloguing data can be found at the end of this publication

Luxembourg: Office for Official Publications of the European Communities, 1996

ISBN 92-827-7122-9

© ECSC-EC-EAEC, Brussels • Luxembourg, 1996

Reproduction is authorized, except for commercial purposes, provided the source is acknowledged

*Printed in Luxembourg*

## **SURFACE INSPECTION OF HOT BARS DURING ROLLING**

British Steel plc

ECSC Agreement No. 7210.GB/806

### **SUMMARY**

The traditional method of inspecting the surface of hot steel bar has been to use surrounding coil eddy-current techniques which have inherent deficiencies. These systems of inspection are insensitive to long seam defects and also transverse defects and are generally limited to bars which are less than 75 mm in diameter. The object of this ECSC project is to develop an alternative method that can overcome these deficiencies and extend the range of bar sizes that can be tested.

The development of water cooled inspection probe assemblies which are capable of being grouped around the bar circumference and the development of very stable electronics for signal processing have been the key features associated with the success of this project.

Plant trials with a five channel inspection head confirmed the defect detection capability and the excellent signal-to-noise ratios suggest that defect detection limits may well be improved down to the 0.5mm level.

These developments indicate that an improved method of hot bar inspection is now entirely feasible which overcomes the major deficiencies of existing bar testing installations.

A proposal for a fully-engineered prototype has been submitted as an ECSC Demonstration Project for installation at the Thybergh Works of UES Steels.



<b>CONTENTS</b>	<b>PAGE</b>
1. INTRODUCTION	1
2. REVIEW OF DETECTION PARAMETERS	1
2.1 Coil Winding Material	2
2.2 Coil Construction	2
2.3 Coil Protection	2
2.4 Coil Characteristics	2
3. RESONANT PROBE TECHNIQUE	3
3.1 Plant Trials	3
3.2 Lift-Off Cancellation	4
3.3 Conveyor Induced Cyclic Variations	4
3.4 Furnace Induced Cyclic Variations	4
3.5 Coil Cooling	4
3.6 Mechanical Considerations	4
4. PHASE SENSITIVE BRIDGE TECHNIQUE	5
4.1 System Description	5
4.2 Automatic Lift-Off Cancellation	5
4.3 Five Channel Inspection System	6
4.4 Production Trials	6
4.5 Analysis of Trial Results	6
5. DISCUSSION OF INSPECTION SYSTEM FEATURES	7
5.1 Product Features	7
5.2 Inspection Features	7
5.3 Engineering Features	8
5.4 Inspection System Costs	8
6. CONCLUSIONS	8
REFERENCES	9
TABLES	10
FIGURES	13

## **LIST OF TABLES**

1. **Properties of Ceramic Materials for Hot Bar Inspection**
2. **Typical Parameters for a Single Inspection Coil (Copper Winding)**
3. **Typical Parameters for a Single Inspection Coil (Constantan Winding)**
4. **Typical parameters for a Dual Coil Detection Probe (Constantan Wire)**



## **LIST OF FIGURES**

1. 10 mm Diameter Test Coil with Copper Winding - Impedance Change for a 70°C Temperature Depression
2. 10 mm Diameter Test Coil with Constantan Winding - Impedance Change for a 70°C Temperature Depression
3. Single 10 mm Diameter Test Coil - 1 mm Defect in Titanium Alloy Bar (Showing Vertical Movement)
4. Single 10 mm Diameter Test Coil - 1 mm Defect in Titanium Alloy Bar (Showing Lateral Movement)
5. Block Diagram of Resonant Probe Concept
6. Interaction of Adjacent Probes Subject to Vertical and Lateral Lift-Off
7. Probe Commutation Sampling Sequence (Not employed in final design)
8. 2 Probe Commutation System
9. Hot bar Inspection Signals Using Cancellation Factor Based on Hot Steel Bar
10. Hot Bar Inspection Signals Using Cancellation Factor Based on Titanium Alloy Bar
11. Bar Temperature Profiles During Hot Bar Trials
12. Variations in Test Coil Temperature During Hot Bar Trials
13. Electronic Signal Processing
14. Relationship Between Voltage Change During Probe Application and Voltage Change for a 0.5 mm and 1.0 mm Defect
15. Processed Defect Output with Delayed Lift-Off Cancellation
16. Relationship Between In-Phase and Quadrature Components During Probe Application
17. Definition of Terms Used in Lift-Off Cancellation
18. Exploded View of Inspection Coil Assembly
19. Local and Remote Electronic Signal Processing Units
20. Test Head Assembly During Installation
21. Test Head Assembly During Production Trials
22. Eddy-Current Inspection Results for Prime Production Bar
23. Eddy-Current Inspection Results for Defective Trial Bar
24. Typical Macro photographs of the Nominal 1.2 mm Defective Zone
25. Typical Macro photographs of the Nominal 2.4 mm Defective Zone

26. **Plots of Defect Output and Probe Temperature v Time During Repeated Traverse of the Calibration Notch in Hot Steel with Unlagged Leads**
27. **Plots of Defect Output and Probe Temperature v Time During Repeated Traverse of the Calibration Notch in Hot Steel with Lagged Leads**
28. **Defect Responses from Resistively Heated Samples**
29. **Macrophotographs of Resistively Heated Defect Samples**
30. **Macrophotographs of Resistively Heated Defect Samples**

## CONTROLE DE LA SURFACE DES BARRES CHAUDES EN COURS DE LAMINAGE

British Steel plc

Accord ECSC n° 7210.GB/806

### RÉSUMÉ

La méthode traditionnelle de contrôle de la surface des barres d'acier chaudes fait intervenir les techniques de sondage par courants de Foucault à bobines encerclantes qui présentent des imperfections inhérentes. Ces systèmes de contrôle ne prennent pas en compte les repliures de laminage ni les criques transversales et se limitent généralement aux barres de moins de 75 mm de diamètre. Ce projet ECSC a pour objet de mettre au point une autre méthode permettant de parer à ces insuffisances et d'élargir la gamme des dimensions de barres pouvant être contrôlées.

La mise au point de sondes de contrôle à refroidissement par eau pouvant être regroupées autour de la circonférence de la barre et le développement d'équipement électronique très stable pour effectuer le traitement des signaux sont les facteurs clefs qui ont contribué au succès de ce projet.

Les essais en usine utilisant une tête de contrôle à cinq canaux ont confirmé la capacité de détection des défauts et les rapports signal/bruit excellents suggèrent qu'il est fort probable que les limites de détection des défauts soient encore améliorées pour atteindre un niveau de 0,5 mm.

Ces développements indiquent qu'une méthode perfectionnée de contrôle des barres chaudes surmontant les principales imperfections des installations de contrôle des barres existantes est à présent tout à fait envisageable.

Une proposition de prototype avec étude technique entièrement terminée a été soumise comme Projet de Démonstration ECSC en vue d'une installation à l'aciérie Thybergh de UES Steels.

TABLE DES MATIERES	PAGE
1. INTRODUCTION	1
2. ETUDE DES PARAMETRES DE DETECTION	1
2.1 Matériau utilisé pour la fabrication des bobines encerclantes	2
2.2 Réalisation des bobines encerclantes	2
2.3 Protection des bobines encerclantes	2
2.4 Caractéristiques des bobines encerclantes	2
3. TECHNIQUE UTILISANT UNE SONDE RESONANTE	3
3.1 Essais en usine	3
3.2 Variation de «lift-off» à l'intérieur de la sonde (lift-off = distance entre la sonde et la surface contrôlée)	4
3.3 Permutations cycliques provoquées par la table à rouleaux	4
3.4 Permutations cycliques provoquées par le four	4
3.5 Refroidissement des bobines encerclantes	4
3.6 Considérations d'ordre mécanique	4
4. TECHNIQUE DU PONT DE MESURE SENSIBLE A LA PHASE	5
4.1 Description du système	5
4.2 Variation automatique de «lift-off»	5
4.3 Tête de contrôle à cinq canaux	6
4.4 Essais de production	6
4.5 Analyse des résultats d'essais	6
5. DISCUSSION DES CARACTERISTIQUES DU SYSTEME DE CONTROLE	7
5.1 Caractéristiques du produit	7
5.2 Caractéristiques de contrôle	7
5.3 Caractéristiques techniques	8
5.4 Coûts du système de contrôle	8
6. CONCLUSIONS	8
REFERENCES	9
TABLES	10
FIGURES	13

## **LISTE DES TABLES**

1. Propriétés des matières céramiques pour le contrôle des barres chaudes
2. Paramètres type pour une bobine de contrôle unique (Enroulement en cuivre)
3. Paramètres type pour une bobine de contrôle unique (Enroulement en constantan)
4. Paramètres type pour une sonde de détection à bobine double (Fil de chauffage en constantan).

## LISTE DES FIGURES

1. Bobine d'essai de 10 mm de diamètre à enroulement en cuivre - Changement d'impédance correspondant à une baisse de température de 70°C
2. Bobine d'essai de 10 mm de diamètre à enroulement en constantan - Changement d'impédance correspondant à une baisse de température de 70°C.
3. Bobine d'essai unique de 10 mm de diamètre - Défaut de 1 mm sur une barre en alliage de titane (Indiquant un mouvement vertical)
4. Bobine d'essai unique de 10 mm de diamètre - Défaut de 1 mm sur une barre en alliage de titane (Indiquant un mouvement latéral)
5. Schéma fonctionnel du concept de la sonde résonnante
6. Interaction des sondes adjacentes soumises au «lift-off» vertical et latéral
7. Séquence d'échantillonnage de commutation des sondes (n'est pas employée dans la réalisation définitive)
8. Système de commutation à deux sondes
9. Signaux de contrôle de la barre chaude utilisant le facteur de variation du «lift-off» sur une barre d'acier chaude
10. Signaux de contrôle de la barre chaude utilisant le facteur de variation du «lift-off» sur une barre en alliage de titane
11. Profil des températures des barres au cours des essais sur barres chaudes
12. Variations de la température de la bobine d'essai au cours des essais sur barres chaudes
13. Traitement des signaux électroniques
14. Relation entre la variation de tension pendant l'application de la sonde et le variation de tension pour un défaut de 0,5 mm et un défaut de 1,0 mm
15. Signal de sortie de défaut traité avec variation de «lift-off» retardée
16. Relation entre la composante en phase et la composante transversale pendant l'application de la sonde
17. Définition des termes utilisés dans la variation de «lift-off».
18. Vue éclatée de l'ensemble bobine de contrôle
19. Unités de traitement des signaux électroniques locales et à distance

20. Ensemble tête de contrôle pendant l'installation
21. Ensemble tête de contrôle pendant les essais de production
22. Résultats de sondage par courants de Foucault obtenus sur une barre de production principale
23. Résultats de sondage par courants de Foucault obtenus sur une barre d'essai défectueuse
24. Macrophotographies caractéristiques de la zone défectueuse nominale de 1,2 mm
25. Macrophotographies caractéristiques de la zone défectueuse nominale de 2,4 mm
26. Graphes du signal de sortie de défaut et de la température de la sonde par rapport au temps pendant le va et vient répété de l'entaille d'étalonnage dans l'acier chaud avec des fils électriques non isolés
27. Graphes du signal de sortie de défaut et de la température de la sonde par rapport au temps pendant le va et vient de l'entaille d'étalonnage dans l'acier chaud avec des fils électriques isolés
28. Défauts obtenus sur les échantillons chauffés par résistance
29. Macrophotographies d'échantillons défectueux chauffés par résistance
30. Macrophotographies d'échantillons défectueux chauffés par résistance





## Prüfung der Oberfläche von Warmstäben während des Walzens

British Steel plc

EGKS Vertrag Nr. 7210.GB/806

### Zusammenfassung

Traditionell hat man für die Prüfung der Oberfläche von Warmstahlstäben Wirbelstromtechniken mit umgebenden Wicklungen benutzt, aber diese Methode hat inhärente Mängel. Diese Prüfsysteme sind unempfindlich gegen lange Nahtdefekte und auch gegen Querdefekte, aus dem Grunde sind sie allgemein auf Stäbe mit einem Durchmesser von weniger als 75 mm begrenzt. Das Ziel dieses EGKS-Vorhabens hat die Entwicklung einer alternativen Methode betroffen, mit der man diese Mängel überwinden und den Bereich der zu prüfenden Stababmessungen erweitern kann.

Die Entwicklung wassergekühlter Sonden­gruppen, die an allen Seiten der Stabperipherie gruppiert werden können, und die Entwicklung sehr stabiler Elektroniksysteme für Signalverarbeitung sind die mit dem Erfolg dieses Vorhabens verbundenen Schlüsselmerkmale gewesen.

Versuche mit einem Fünfkana­l-Prüfkopf im Werk haben das Defektnachweisvermögen bestätigt, und die ausgezeichneten Störabstände legen nahe, daß die Defektnachweisbegrenzungen sehr wahrscheinlich auf ein Niveau von 0,5 mm reduziert werden können.

Diese Entwicklungen deuten an, daß eine bessere Methode für Prüfung von Warmstäben heute durchaus möglich ist, mit der man die Hauptmängel existierender Stabtestanlagen überwinden kann.

Man hat einen Antrag für einen großtechnischen Prototyp als ein EGKS-Vorhaben für Vorführungszwecke zum Einbau im Thrybergh-Werk der Firma UES-Steels vorgelegt.

Inhaltsverzeichnis	Seite
1. Einleitung	1
2. Überblick der Nachweisparameter	1
2.1 Spulenwicklungswerkstoff	2
2.2 Spulenkonstruktion	2
2.3 Spulenschutz	2
2.4 Spulencharakteristika	2
3. Resonanzsondentechnik	3
3.1 Versuche im Werk	3
3.2 Abstandsannullierung	4
3.3. Förderbandinduzierte zyklische Schwankungen	4
3.4 Ofeninduzierte zyklische Schwankungen	4
3.5 Spulenkühlung	4
3.6 Mechanische Erwägungen	4
4. Phasenempfindliche Brückentechnik	5
4.1 Systembeschreibung	5
4.2 Automatische Abstandsannullierung	5
4.3 Fünfkanal-Prüfsystem	6
4.4 Produktionsversuche	6
4.5 Analyse der Versuchsergebnisse	6
5. Diskussion der Prüfsystemmerkmale	7
5.1 Produktmerkmale	7
5.2 Prüfmerkmale	7
5.3 Technische Merkmale	8
5.4 Prüfsystemaufwand	8
6. Schlußfolgerungen	8
Literaturverzeichnis	9
Tabellen	10
Abbildungen	13

## Aufstellung der Tabellen

1. Eigenschaften des Keramikmaterials für die Prüfung von Warmstäben
2. Typische Parameter für eine Prüfspule (Kupferwicklung)
3. Typische Parameter für eine Prüfspule (Constantan-Wicklung)
4. Typische Parameter für eine Sonde mit Doppelspule (Constantan-Draht)

## Aufstellung der Abbildungen

1. 10 mm Durchmesser-Testspule mit Kupferwicklung - Impedanzveränderung für eine 70<sup>0</sup>C Temperatursenkung
2. 10 mm Durchmesser-Testspule mit Constantanwicklung - Impedanzveränderung für eine 70<sup>0</sup>C Temperatursenkung
3. Eine 10 mm Durchmesser-Testspule - 1 mm Defekt im Titanlegierungsstab (zeigt die vertikale Bewegung)
4. Eine 10 mm Durchmesser-Testspule - 1 mm Defekt im Titanlegierungsstab (zeigt die seitliche Bewegung)
5. Blockdiagramm der Resonanzsondenkonzeption
6. Wechselwirkung benachbarter Sonden, die dem vertikalen und seitlichen Abstand ausgesetzt sind
7. Probenahmefolge der Sondenkommutation (nicht in der endgültigen Konstruktion ausgenutzt)
8. 2-Sondenkommutationssystem
9. Warmstab-Prüfsignale verwenden den auf den Warmstahlstab gestützten Annullierungsfaktor
10. Warmstab-Prüfsignale verwenden den auf den Titanlegierungsstab gestützten Annullierungsfaktor
11. Stabtemperaturprofile während der Warmstabversuche
12. Veränderung der Testspulentemperatur während der Warmstabversuche
13. Verarbeitung der elektronischen Signale
14. Beziehung zwischen der Spannungsveränderung während des Sondereinsatzes und der Spannungsveränderung für einen 0,5 mm und 1,0 mm Defekt
15. Verarbeitete Defektausgabe mit verzögerter Abstandsannullierung
16. Beziehung zwischen den gleichphasigen Komponenten und denen mit 90<sup>0</sup>. Phasenverschiebung während des Sondereinsatzes
17. Definition der in der Abstandsannullierung benutzten Begriffe
18. Darstellung in auseinandergezogener Anordnung der Prüfspulengruppe
19. Lokale und Fernverarbeitungseinheiten der elektronischen Signale
20. Testkopfgruppe während der Installation
21. Testkopfgruppe während der Produktionsversuche
22. Wirbelstromprüfergebnisse für den Hauptproduktionsstab
23. Wirbelstromprüfergebnisse für den defekten Versuchsstab
24. Typische Makroaufnahmen der nominal 1,2 mm defekten Zone
25. Typische Makroaufnahmen der nominal 2,4 mm defekten Zone
26. Kurven der Defektausgabe und Sondentemperatur gegen die Zeit während der wiederholten Eicheinkerbung in der Querrichtung im Warmstahl mit nichtverkleideten Kabeln
27. Kurven der Defektausgabe und Sondentemperatur gegen die Zeit während der wiederholten Eicheinkerbung in der Querrichtung im Warmstahl mit verkleideten Kabeln
28. Defektreaktionen von den widerstandserwärmten Probestücken
29. Makroaufnahmen der widerstandserwärmten, defekten Probestücke
30. Makroaufnahmen der widerstandserwärmten, defekten Probestücke

# **SURFACE INSPECTION OF HOT BARS DURING ROLLING**

British Steel plc

ECSC Agreement No. 7210.GB/806

## **FINAL TECHNICAL REPORT**

### **1. INTRODUCTION**

Traditional hot bar inspection systems have employed the surrounding-coil eddy-current inspection technique. This technique has fundamental defect detection limitations and these limitations have had to be tolerated by production plant in the absence of more refined methods. This surrounding-coil detection system cannot adequately resolve longitudinal seam defects unless they are short in length because of the differential action of the detection coils. In addition, defects which are purely circumferential in nature do not disturb the flow of the eddy currents and are also not detectable. There is clearly a need for an improved detection system which can overcome these shortcomings.

The purpose of this project was to develop an improved eddy-current technique for the in-line inspection of hot bar surfaces at rolling temperatures for the presence of longitudinal seam defects.

The optimum siting for a hot bar inspection system would be a position downstream of the final sizing pass before significant scale formation can take place and prior to any water quenching treatment which can lower the bar below the Curie temperature and make eddy-current inspection impractical.

The trial site at the Thrybergh Works of UES Steels included a Koch's precision sizing block and the inspection unit was located immediately downstream of this sizing block taking advantage of the excellent inherent guidance features.

The proposed inspection technique depended on the grouping of individual water-cooled probe coils around the circumference of the hot bar. These coil assemblies were mounted on ceramic wear plates which contacted the bar surface to establish the correct operating clearances and acted in an absolute detection mode to allow the detection of longitudinal and transverse bar defects. This success of this project was very much conditioned by the development and optimisation of the inspection probe assemblies and also the associated processing electronics with due regard for the bar size range rolled on this particular mill.

### **2. REVIEW OF DETECTION PARAMETERS**

The use of single or dual excitation frequencies, the variations in the size and type of coil construction, the choice of coil construction materials and electronic processing methods all need to be optimised if the development programme is to be successful.

The successful detection of longitudinal defects implies absolute processing techniques and to obtain adequate defect detection sensitivity it is necessary to reduce the search area associated with each detection coil. An array of probe coils distributed around the product circumference provides a good basis for the design of a detection head assembly provided that the problems of sensitivity and overall stability can be resolved.

Dual frequency methods were examined early in the project but it was soon recognised that, with multiple coil inspection heads, the sheer volume of processing electronics would be unwieldy, expensive and would offer no real advantage over the simpler single frequency methods.

The choice of a single operating frequency should take due consideration of defect processing rates and offer good separation of defect information from lift-off effects. The phase angle separation between defect and lift-off vectors increases with test frequency and a practical operating frequency of 1 MHz was adopted.

## **2.1 Coil Winding Material**

It became apparent in the early stages of the development programme that coil stability, at these enhanced operating sensitivities, was critical to the success of the project if defect signals were not to be masked by coil temperature variations. This is illustrated in the impedance plane diagram of Fig. 1 where the effects of a temperature change of 70 degrees Celsius on a coil wound with copper wire can be seen. This change was much larger than the signal produced by a 1 mm defect and would therefore impose a significant limit on defect detectability. A range of alternative coil materials was evaluated and Constantan was selected as being the most effective in reducing temperature effects. The impedance plane diagram shown in Fig. 2 indicates the measure of improvement obtained when a Constantan coil was subjected to the same temperature change. The coil temperature effects have been reduced by a factor of at least 30 by using Constantan wire and this coil material was used for all subsequent coil assemblies.

## **2.2 Coil Construction**

Trials were also undertaken with various coil constructions to optimise the recovered defect signal relative to signals produced by variations in coil operating clearance, commonly referred to as the lift-off effect. Dual coil assemblies were examined and included orthogonal, dual-D and concentric coil configurations. The only configuration that showed any promise was the concentric coil arrangement but the overall coil size was large in relation to the sensing area and the coil construction was significantly more complicated. These are important factors where multiple coil test head assemblies are envisaged and this arrangement was therefore rejected. The examination of single coil assemblies was restricted to a single cylindrical coil of 10 mm diameter and two radially displaced coils of similar dimensions. The two radial coils offered reasonable rejection of lift-off and thermal effects but were very sensitive to lateral movement of the bar and also effects of coil tilt and, for these reasons, were discounted. The single cylindrical coil offered reasonable coverage and constructional simplicity but required the use of phase sensitive detection for lift-off cancellation. The single coil configuration was adopted to ensure that the engineering complexity of inspection head assembly was minimised.

## **2.3 Coil Protection**

The coil assembly is designed to slide on the bar surface to provide a controlled coil clearance and the selection of a suitable facing material is an important feature in the design. The detection coil is contained in a water cooled housing faced by a ceramic shoe. Water is directed through the centre of the coil and issues through the narrow annulus between the end of the coil and the ceramic facing material into the outer collection chamber. Under normal operating conditions one side of the 2.25 mm thick ceramic facing will be in contact with the bar at 1100 degrees celsius and the other side will be in contact with cooling water at around 20 degrees celsius. The selection of a suitable ceramic will therefore depend predominantly on its ability to withstand thermal shock and also to tolerate the high thermal gradient across the thin wall section. Table 1 lists the properties of some ceramic materials that have been considered. Silicon nitride exhibits the highest thermal shock resistance and can be machined at the green stage to produce a well toleranced component. Experience with this material during hot bar trials has confirmed its suitability for this purpose and it showed negligible wear over a period of several hours. This ceramic is also resistant to metal pick-up when in contact with molten metals and can be obtained in a glazed form to resist water absorption, which can produce breakup of the ceramic resulting from the rapid formation of steam.

## **2.4 Coil Characteristics**

Tables 2, 3 and 4 illustrate typical coil characteristics for the two principle coil constructions considered when applied to both steel and titanium alloy test samples. The titanium test sample was selected as being similar in properties to steel at rolling temperatures. The changes in test conditions from cold steel

to hot steel, as typified by the titanium alloy sample bar, incurs a loss in sensitivity of 5:1. The use of Constantan wire for the winding produces a further loss of 3:2 giving an overall loss of 15:2. With the dual coil arrangement an additional loss of 2:1 would be experienced.

The dynamic response of the preferred 10 mm diameter single cylindrical test coil is illustrated in Figs. 3 and 4. Figure 3 shows the lift-off cancellation that can be achieved by a vector rotation of 88 degrees when the coil traverses a 1 mm defect at the three specified operating clearances. The lift-off residual can be reduced even further in a practical design by allowing smaller increments in rotation than the test instrumentation limit of 1 degree. Figure 4 indicates the tolerance to lateral bar movement for displacements of  $\pm 0.5$  mm.

### **3. RESONANT PROBE TECHNIQUE**

The test coil was initially incorporated as a tuned element in an oscillatory circuit and the reactive and resistive components were extracted by decoding the frequency and amplitude information as shown in Fig. 5. The subsequent combination of these two channels has the same effect as phase rotation in producing lift-off cancellation. Initial tests were conducted on a group of three probes but it soon became evident that probe interactions were taking place as the oscillators attempted to lock depending on their harmonic relationships - these effects can be observed in Fig. 6. It was not possible to eliminate this interaction and the use of probe commutation techniques was examined. With this technique each probe is activated in sequence allowing time for the output signal to stabilise before a reading was taken. Figure 7 shows the timing relationships and the resultant waveforms for two probes commutated at 1 kHz is shown in Fig. 8. Increased background noise was produced with this method because of interaction between the switching waveforms and the oscillator circuit caused by capacitive feedthrough and also steps in the output waveform could be observed due to asynchronous switching of the oscillator. For these reasons and because the sampling technique would only allow each coil to sample the bar at around 15mm intervals at bar speeds of 15 m/s the concept was discarded.

#### **3.1 Plant Trials**

The resonant probe technique was used to assess detection performance on hot bar at rolling temperatures with a single cylindrical test coil. The test coil was constructed along the lines discussed earlier, contained in a water cooled metal housing, and then cemented to a long silicon nitride shoe which rode on the surface of the hot bar. The probe assembly was applied to the bar with a trailing parallelogram linkage to ensure that the probe facing was maintained parallel to the bar surface during its application and retraction. The probe was applied to and retracted from the bar surface using a pneumatic cylinder.

The trial was conducted at the Thrybergh works of United Engineering Steels and the test unit was located immediately downstream of the Kochs precision sizing block which gave good control of the bar position on exit. The space available at this point in the line constrained the overall length of the test head to approximately 200 mm.

Coil cooling was provided by a peristaltic pump fed from a separate water tank at a cooling flow rate of around 7 litres/min.

The trials were restricted to bar sizes in excess of 50 mm to avoid problems associated with bar droop within the test head zone.

The two outputs from the probe channel were monitored on a multichannel FM tape recorder system to allow subsequent analysis. Coil temperature was measured by sensing the output voltage from a thermistor embedded in the coil winding and bar temperature variations along the bar were monitored with a hand-held two-colour optical pyrometer which provided an electrical output for recording purposes.

The object of this trial was to establish the suitability of the engineering materials in a practical production environment and, at the same time, to monitor the processed results from a single eddy current channel to ensure that no unexpected inspection problems were encountered.

### **3.2 Lift-Off Cancellation**

The traces shown in Fig 9 are typical of the recordings obtained from the coil during test. The top trace relates to coil inductive variations, the middle trace relates to coil resistive variations and the lower trace represents the final output signal after combining the two traces in the optimum ratio and applying amplification.

The underlying cyclic lift-off variations have been cancelled to good effect leaving a good datum against which to judge any defect content. Defect signals would normally be positive in polarity and the unexpected negative signal peak seen on the output trace was eventually traced to a malfunction in the tape recording system. This spurious signal occurred randomly throughout the tape recordings but, since no comparisons were being made at this stage with cold bar inspection results, this effect did not present any real problems.

The same signal recordings were then combined in the ratio which would give optimum rejection of lift-off effects based on the use of the titanium alloy reference bar which had been judged to be close in properties to that of a hot steel bar. It is evident from the results shown in Fig 10 that the titanium alloy bar cannot be used to provide the correct cancellation factor for in-line operation and it is essential that some other means must be found of determining the correct factor, to allow the resolution of harmful defects. It may be possible to use the application of the test head onto the hot bar as a means of determining the optimum cancellation ratio on a bar by bar basis.

### **3.3 Conveyor Induced Cyclic Variations**

There is an underlying cyclic variation present on both the traces shown in Figs. 9 and 10. Further investigation showed a strong correlation between these cyclic signals and the time interval between rollers on the conveyor and therefore it has been assumed that the signals are induced by the motion of the bar nose over individual rollers along the roller table. This behaviour further endorses the need to have good lift-off cancellation as a design feature.

### **3.4 Furnace Induced Cyclic Variations**

The recordings of bar temperature using the optical two-colour pyrometer shown in Fig. 11 indicate cycles in surface temperature along the length of the bar. After a lot of investigation this was correlated with the positions of the supports within the reheat furnace which appeared to leave cool zones along the length of the bar. The temperature depressions amounted to around 40 degrees Celsius and concern was registered that these effects may produce pseudo defect indications. Examination of other areas of the defect recordings with optimum lift-off rejection did not reveal any irregularities and it must therefore be assumed that variations in surface temperature and lift-off are similar in effect and are rejected together.

### **3.5 Coil Cooling**

The trace shown in Fig. 12 was derived from the thermistor which was embedded within the coil assembly and was obtained during a sequence of bar tests. The initial rise is the result of heating the coil assembly from a cool condition and then the coil temperature profile stabilises and then cycles between 45°C and 50°C as bars enter and exit the test station. Cooling water flow rates of around 7 litres/h were employed with a rise in water temperature of around 20°C. These flow rates indicate that it is necessary to extract approximately 160 W of heat from the probe housing itself to maintain an internal probe temperatures of the order of 50°C. With a configuration of 32 probes in a more practical array a total heat content in excess of 5 kW would need to be extracted to maintain sensible coil temperatures.

### **3.6 Mechanical Considerations**

The probe was located behind a 3 mm thick silicon nitride skid of approximately 100 mm in length and was applied pneumatically using a parallelogram linkage. This proved to be effective and the probe was maintained in contact with the surface at all times. After the trial period in which more than 80 bars had been processed the skid was examined to determine the extent of any wear that may have taken place. No



discernible wear patterns were evident and therefore silicon nitride will continue to be used in all future trials.

#### 4. PHASE SENSITIVE BRIDGE TECHNIQUE

The interaction of oscillatory circuits in multiprobe inspection heads requires the development of alternative electronic signal processing operating at fixed frequency with ultra-stable characteristics.

##### 4.1 System Description

The proposed electronic processing system for multi-channel operation is illustrated in Fig. 13 where all the probes are energised from one single crystal controlled oscillator. Each coil forms part of a bridge circuit which is balanced prior to the application of the probe to the metal surface. Subsequent amplification of the bridge signals is achieved in a very stable video amplifier before being fed to the inputs of phase sensitive detector stages. These phase sensitive detectors must also be very stable in operation because any dc drift that takes place will appear as an additional component in the signal output, either enhancing or suppressing the true defect component depending on the polarity of the voltage drift. The magnitude of the problem can be appreciated by referring to Fig. 14 where the excursion in voltage from the phase detectors in moving the probe onto the test surface has been recorded together with the defect excursions produced by a 0.5 mm and 1.0 mm defect. The resultant defect signal obtained by subtracting these two waveforms in the optimum ratio equates to only 1.5% of the original step height and it will, therefore, be necessary to establish the correct cancellation factor to an accuracy of better than 0.2% to minimise residual lift-off content.

##### 4.2 Automatic Lift-Off Cancellation

The inclusion of accurate automatic lift-off cancellation is a vital step in the development of this inspection system for the reasons mentioned above. Figure 15 illustrates the gross signals that can result from the use of an incorrect cancellation factor on the in-phase and quadrature signal components immediately after probe has been applied onto a hot bar surface compared to the relatively stable datum established thereafter by the use of the correct cancellation factor. These results were generated from previously recorded single-channel phase-detector outputs obtained during earlier hot bar trials. It was determined that the best form of automatic lift-off cancellation was achieved by using the voltage excursions generated by the phase detectors when the probes are applied to the bar surface. The ideal cancellation factor can be derived from the ratio of phase detector voltages with a minor correction factor which depends on surface contour. Figure 16 shows the in-phase and quadrature detector voltage excursions during probe application and the relationship between them over the duration of the application stroke. The incremental slope at the end of the application stroke is close in value to the absolute slope derived over the entire stroke and only minor corrections are required. The definition of terms used in automatic lift-off cancellation can be seen by referring to Fig. 17 which shows idealised application waveforms. The electronic processing ensures that the two wave forms are referenced to 0 V prior to head application. Immediately after probe application the maximum voltage excursions are stored and their ratio is used in the subsequent cancellation process. The voltage changes from these maximum levels are used to indicate defect or lift-off excursions at the normal coil operating clearance of 3 mm. The output signal is derived according to the formula below.

$$\text{Defect Output} = \Delta\phi \times \frac{k \cdot j\phi_{\max}}{\phi_{\max}} - \Delta j\phi$$

A five channel eddy-current processing system was designed along the foregoing lines exercising great care in the design and selection of components to ensure that devices were conservatively rated and offered intrinsically very low levels of voltage drift.

### **4.3 Five Channel Inspection System**

An exploded view of a typical eddy-current coil assembly is shown in Fig. 18 with a circular protective window ceramic window and a water cooled probe housing. A temperature measuring device is embedded close to the water chamber to ensure that cooling water flow rates are adequate. The main housing is faced with ceramic in the areas which are in contact with the bar surface.

Figure 19 shows the processing electronics developed for this trial and for technical reasons this had to be separated into a small enclosure which had to be mounted adjacent to the inspection head containing the high frequency bridge and phase detectors and a larger remote enclosure containing the remainder of the processing electronics including the automatic lift-off cancellation.

The inspection head was comprised of five eddy-current coil assemblies mounted in pantograph assemblies which were applied to the bar surface by means of pneumatic cylinders. Figure 20 shows the general construction of inspection head at the point of installation and Fig. 21 shows the unit in operation on the mill during production trials.

### **4.4 Production Trials**

The inspection head was sited immediately downstream from the Koch's precision sizing block on the production line of the Thrybergh Bar Mill at UES Steels in Rotherham. The five probe channels allowed the inspection of one quarter of the surface of a 68 mm diameter bar. It was obviously important to ensure that defective material would pass under this close grouping of probes and that was accomplished by obtaining a prime billet of 140 mm section and machining artificial defects of known depth into all four billet faces at two zones along the 13 m length. At the first zone, a defect of 6 mm depth was machined at an angle across each face of the billet for a distance of approximately 1 m. At the second zone, the defects were similarly introduced but at the reduced depth of 3 mm. The positions of the defective zones were selected so that each of the zones would be contained in individual bar lengths of nominally 8 m.

The billet was reheated and rolled to 68 mm diameter bar and inspected with the five channel head assembly which was calibrated using a 1 mm defect standard in an austenitic bar; trials with resistively heated samples had already shown that hot steel bars and cold austenitic steel bars had comparable properties. Full monitoring of all output signals was achieved by using FM tape recorders and high speed event recorders.

The trial material was included at the end of a normal production run on the same bar size so an opportunity was taken to inspect material that should be of prime quality. The traces in Fig. 22 show the responses from each of the five probe channels on this production material. It will be noticed that some drift is evident over the full length of the bar but no measurable defect content was registered. The next bar was the trial bar with the two defective zones and the test results are shown in Fig. 23. The two defective areas showed up clearly on all five probe channels exhibiting excellent signal-to-noise ratios but the signal drift that was observed on the previous bar was still present. The second zone on probe channel 3 showed two separate indications where the probe was travelling down the bar in a position which corresponded to the original billet corner and where the billet face defects adjacent to that corner produced marginal responses.

### **4.5 Analysis of Trial Results**

The trial bars containing the two defective zones were hand probed with conventional eddy-current equipment and the positions of the seams were marked. The bars were then sectioned at each of the two defective zones and classic longitudinal seams of nominally 1.2 mm and 2.4 mm were observed on the macrophotographs. Figure 24 shows the four 1.2 mm defects at a magnification of x 34 and Fig. 25 shows the four 2.4 mm defects at the same magnification. These results were very encouraging and suggest that defect detection sensitivities down to 0.5 mm may be practical.

Detailed tests were conducted on the inspection head assembly to determine the cause of the signal drift on the output waveforms. Eventually it was found that the radiant heating of the coil coaxial leads was

predominantly responsible for this behaviour. In a final system design this problem can be overcome by routing the connecting leads through water cooled jackets and avoiding direct radiation paths wherever possible. Figure 26 illustrates the drift in signal output experienced during testing of a resistively heated austenitic calibration tube with a probe cooling water flow rate of nominally 0.1 litres/min with no protection against radiant heating. The corresponding traces shown in Fig. 27 show no significant drift when the connecting leads were lagged against the radiant heat coming from the hot tube. This test confirmed that little problem should be experienced with thermal drift providing good engineering construction practices are observed.

## **5. DISCUSSION OF INSPECTION SYSTEM FEATURES**

The multiple probe head assembly responded well to longitudinal seams of the order of 1 mm in depth and the noise levels experienced on these trials suggest that defect detection capability might well be improved to the 0.5 mm level. These absolute detection levels are a feature of the probe coil technique and do not relate to the diameter of the bar. This allows improved inspection performance on larger bar diameters (when expressed as a percentage of bar diameter) but can be a limiting feature on small bar sizes where increased sensitivities are desirable. The following sections discuss the features of this new development and the implications of including this form of inspection system in a hot bar production line.

### **5.1 Product Features**

Good bar guidance is an essential pre-requisite for success with this method of inspection and it will be necessary to maintain the bar position within the inspection zone to better than 2 or 3 mm of an ideal bar centreline in all planes.

It will be necessary to make provision for retaining the Koch's block in-line for all bar sizes to ensure adequate guidance is obtained throughout the production range.

The probe development has been optimised for operation over the round-bar size range rolled at Thrybergh (15 mm to 110 mm). Further probe development may well be required for reduced bar diameters.

The inspection of square or hexagonal products, whilst being a feasible proposition, would require careful thought in the design of the test head to allow for the variety of product sections and would also put constraints on the bar rotation through the inspection area; a problem not encountered in round bar testing.

The presence of excessive water on the bar surface immediately prior to test can cause spurious defect information to be generated particularly if the surface temperature is caused to reduce below Curie point. All eddy-current systems are vulnerable to this effect and encircling coil systems are often preceded by an air-knife to minimise the problem.

Scale build-up can interfere with the detection action because scale can cool rapidly below Curie levels and leave a variable magnetic layer on the bar surface. Siting the test head close to mill stand with an air-knife usually effects a cure.

### **5.2 Inspection Features**

The limiting factors on achievable detection sensitivity relate firstly to the disproportionate fall-off in defect signal below 1 mm defect depth (a problem caused by the physics of detection), secondly to the surface condition of the hot bar or surface roughness (sensitivity is usually restricted to three times the surface roughness) and finally to the rejection of lift-off signals in the final defect output (this rejection factor is calculated automatically during probe application).

It has already been mentioned that the probe development was optimised for the range of bar sizes produced at the Thrybergh Mill of United Engineering Steels and the probe sensing area ranges from 6mm to 10mm diameter according to the size of bar being inspected. This coil size represents a compromise

between detection sensitivity level and the number of coils required to cover the surface of the larger bar sizes. With the current coil design approximately 32 coils will need to be accommodated in the largest head assembly.

The probe design is omnidirectional and it should be possible to respond to most orientations of defect. A catalogue of various defect types is being gathered together with the responses that can be obtained. Figure 28 illustrates some trial results obtained from resistively heated bar samples containing natural defects. Responses have been obtained for three bar samples A, B & C and Fig. 29 contains three macrophotographs corresponding to the three defects on bar A at a magnification of x 20. All the defects in Fig. 29 are laps with a surface penetration of only 0.2 mm to 0.4 mm but they have a surface length of 2 mm to 4 mm ensuring good detection. In Fig. 30 the upper and lower macrophotographs relate to bar samples B and C respectively also shown at the same magnification of x 20. Sample B contains a 0.6 mm deep seam defect and sample C has a rough scale-filled area approximately 0.1 mm in depth. A 1 mm calibration defect would produce a 3 division shift relative to the A bar responses and a 6 division shift relative to all other responses. The signals are therefore commensurate with the defect content. The system should be capable of detecting longitudinal and transverse defects within the limits previously mentioned, rolling laps, areas of shell and roll marks which produce significant surface effects. There would be less confidence in picking up shallow surface grooves since these defects would tend to be treated as lift-off changes and would be cancelled accordingly.

### **5.3 Engineering Features**

It has already been mentioned that bar guidance is an important factor and in that context it would be prudent and cost effective to consider the use of the Kochs precision sizing block (PSB) for that purpose. The space is quite restrictive however and a careful design study will need to be made to assess whether the test head assembly can be accommodated within the confines of the PSB. The inspection head could be accommodated in an on-line position interleaved with the limbs of the Kochs block but capable of being retracted off-line for maintenance purposes.

The alternative option is to develop an integrated bar guidance arrangement distributed throughout the inspection system. This will obviously incur a large cost penalty and it would also need to be automatic in its adjustment for varying bar diameter to effect manpower savings. This development should not be undertaken lightly since the concept is difficult to engineer.

It should also be appreciated that if the test coil assemblies are applied after the bar nose has passed then the application time of typically 0.5 s will produce an uninspected end loss related to the speed of the bar. The losses at the tail end of the bar will be significantly less because any retraction delay will keep the inspection head in contact longer.

### **5.4 Inspection System Costs**

It is difficult, without a detailed study, to give a firm idea on the outturn cost for the design of this type of inspection system but it is anticipated that the cost would be of the order of £500 000 if the inspection system were to be incorporated into the PSB. These costs would obviously include the initial electronic and mechanical design and subsequent repeat systems would therefore be correspondingly cheaper. Without a clearer understanding of the design concept for a unit with integral guidance it would not be sensible to speculate on the outturn cost of a fully integrated inspection system.

## **6. CONCLUSIONS**

The successful development of a stable, water-cooled, eddy-current, inspection probe has been an important aspect of this development programme. The provision of a silicon nitride ceramic protective facing has made it possible to contain the cooling water whilst at the same time allowing the probe assembly to slide on the bar surface at a predetermined operating clearance with minimal wear.

The development of ultrastable processing electronics has been an equally important feature of the overall inspection package and will allow the multichannel operation that this technique demands.

The hot bar inspection trials were very successful and good signal-to-noise ratios were obtained on all output signals suggesting that defect detection sensitivities down to 0.5 mm might be possible.

The provision of good bar guidance throughout the length of the inspection head assembly is an essential pre-requisite and costs benefits may well accrue if the guidance features of existing precision sizing blocks are integrated into the head design concepts.

A proposal for a fully-engineered prototype has been submitted as an ECSC Demonstration Project for installation at the Thybergh Works of UES Steels.

## REFERENCES

1. 'Detection of Surface and Subcutaneous Defects in Hot Continuously-Cast Billets by Means of Eddy Current', ECSC Research Contract 7210.GB/305, IRSID, Unimetal.
2. K.G. Bergstrand and P. Nilsson: 'Hot Surface Inspection by a New Eddy-Current Technique', *Iron and Steel Engineer*, January 1980, pp 59-61.
3. S.F. Gerard: 'High Temperature in Eddy-Current Testing of Surface Defects on Steel Wire Rod During Rolling', *Proc. 11th Conference on NDT, Las Vegas, Part 1, 1985*, pp 179-185.
4. T. Stepinski and K.G. Bergstrand: 'Improved Eddy Current Methods in Hot Steel Testing', *Proc. 11th Conference on NDT, Las Vegas, Part 1, 1985*, pp 137-143.
5. T. Stepinski: 'Real Time Signal Analysis in Eddy-Current NDT Equipment', *Proc. 4th European Conference on NDT, 1987*.

**TABLE 1  
PROPERTIES OF CERAMIC MATERIALS FOR HOT BAR INSPECTION**

	Alumina Al <sub>2</sub> O <sub>3</sub>	Silicon Carbide SiC	Silicon Nitride Si <sub>3</sub> N <sub>4</sub>	Boron Carbide B <sub>4</sub> C	Boron Nitride BN
Maximum Temperature, °C Short Term Long Term		1600 1400	1400 1150	1500	1000
Thermal Shock, °C	350	400	650		High
Thermal Expansion, 1/K.10 <sup>6</sup>	8	4	3	5	3
Thermal Conductivity, W/m K @ 20°C @ 1000°C	23	150 45	25 18	38 18	22 11
Density, g/cc	3.9	3.1	3.2	2.5	
Resistivity, Ω m @ 20°C @ 1000°C	10 <sup>12</sup>	10	10 <sup>10</sup> 10 <sup>5</sup>	0.1-10	10 <sup>11</sup>
Tensile Strength, GPa	300	410	290	450	60
Compressive Strength, MPa	2100	2000	2000	2800	
Flexural Strength, MPa @ 20°C @ 1000°C	300	410 410	650 450	400 300	
Hardness, HV, kg/mm <sup>2</sup>	1500	3000	1500	300	3000
Fracture Toughness, MPa √m	4	4	8		
Molten Metal Resistance		Average	Good		Good
Machinability			Green (Unfired State)		Good

**TABLE 2**  
**TYPICAL PARAMETERS FOR A SINGLE INSPECTION COIL**  
**(COPPER WINDING)**

*Steel Test Sample*

Test frequency is 1 MHz  
All parameters are expressed as % of coil impedance  
Defect size is 1 mm in a steel reference block  
Lift-off excursion is  $\pm 0.5$  mm around 3.0 mm nominal  
Coil ID is 10 mm using copper wire  
Defect vector length @ 3 mm LO is 0.215% @ 63°  
Lift-off vector is 1.49% @ 125°  
Included angle is 62 producing a defect factor of 0.883  
Residual defect at 2.5 mm LO is 0.245% after cancellation  
Residual defect at 3.0 mm LO is 0.192% after cancellation  
Residual defect at 3.5 mm LO is 0.128% after cancellation  
Residual lift-off is 0.032% after cancellation

*Titanium Test Sample*

Test frequency is 1 MHz  
All parameters are expressed as % of coil impedance  
Defect size is 1 mm in a titanium alloy bar  
Lift-off excursion is  $\pm 0.5$  mm around 3.0 mm nominal  
Coil ID is 10 mm using copper wire  
Defect vector length @ 3 mm LO is 0.11% @ 64°  
Lift-off vector is 2.08% @ 95°  
Included angle is 21 producing a defect factor of 0.358  
Residual defect at 2.5 mm LO is 0.053% after cancellation  
Residual defect at 3.0 mm LO is 0.037% after cancellation  
Residual defect at 3.5 mm LO is 0.027% after cancellation  
Residual lift-off is 0.021% after cancellation

**TABLE 3**  
**TYPICAL PARAMETERS FOR A SINGLE INSPECTION COIL**  
**(CONSTANTAN WINDING)**

*Titanium Test Sample*

Test frequency is 1 MHz  
All parameters are expressed as % of coil impedance  
Defect size is 1 mm in a titanium alloy bar  
Lift-off excursion is  $\pm 0.5$  mm around 3.0 mm nominal  
Coil ID is 10 mm using constantan wire  
Defect vector length @ 3 mm LO is 0.065% @ 86°  
Lift-off vector is 0.645% @ 108°  
Included angle is 22 producing a defect factor of 0.365  
Residual defect at 2.5 mm LO is 0.036% after cancellation  
Residual defect at 3.0 mm LO is 0.028% after cancellation  
Residual defect at 3.5 mm LO is 0.022% after cancellation  
Residual lift-off is 0.007% after cancellation

**TABLE 4**  
**TYPICAL PARAMETERS FOR A DUAL COIL DETECTION PROBE**  
**(CONSTANTAN WIRE)**

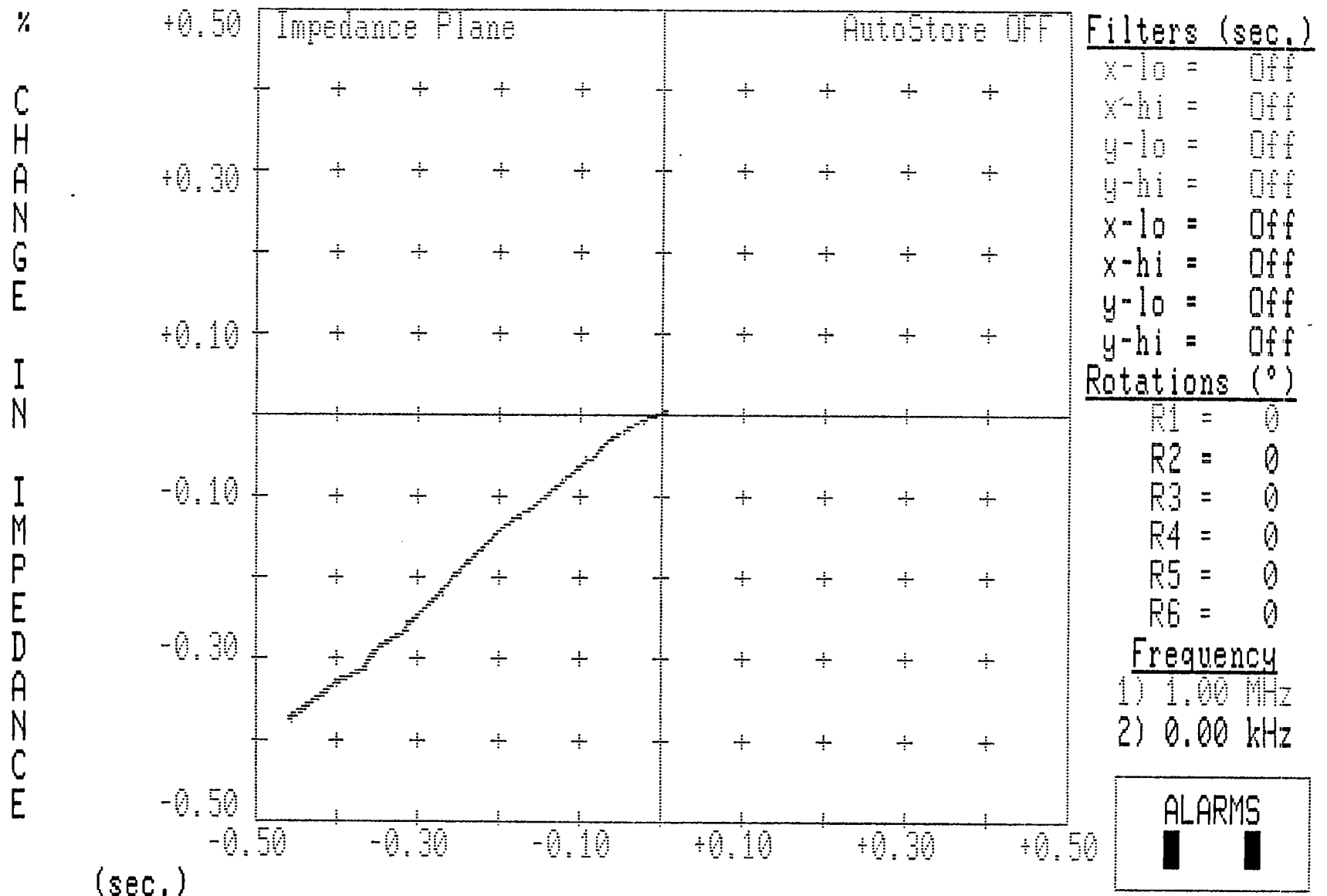
*Steel Test Sample*

Test frequency is 1 MHz  
All parameters are expressed as % of coil impedance  
Defect size is 1 mm in a steel reference block  
Lift-off excursion is  $\pm 0.5$  mm around 3.0 mm nominal  
Coil ID's of 5 mm and 13 mm using constantan wire  
Defect vector length @ 3 mm LO is 0.075% @ 90°  
Lift-off vector is 0.27% @ 180°  
Included angle is 90 producing a defect factor of 1.000  
Residual defect at 2.5 mm LO is 0.128% after cancellation  
Residual defect at 3.0 mm LO is 0.075% after cancellation  
Residual defect at 3.5 mm LO is 0.038% after cancellation  
Residual lift-off is  $\leq 0.012\%$  after cancellation

*Titanium Test Sample*

Test frequency is 1 MHz  
All parameters are expressed as % of coil impedance  
Defect size is 1 mm in a titanium alloy bar  
Lift-off excursion is  $\pm 0.5$  mm around 3.0 mm nominal  
Coil ID's of 5 mm and 13 mm using constantan wire  
Defect vector length @ 3 mm LO is 0.036% @ 98.0°  
Lift-off vector is 0.26% @ 117°  
Included angle is 19 producing a defect factor of 0.333  
Residual defect at 2.5 mm LO is 0.022% after cancellation  
Residual defect at 3.0 mm LO is 0.012% after cancellation  
Residual defect at 3.5 mm LO is 0.007% after cancellation  
Residual lift-off is  $\leq 0.002\%$  after cancellation

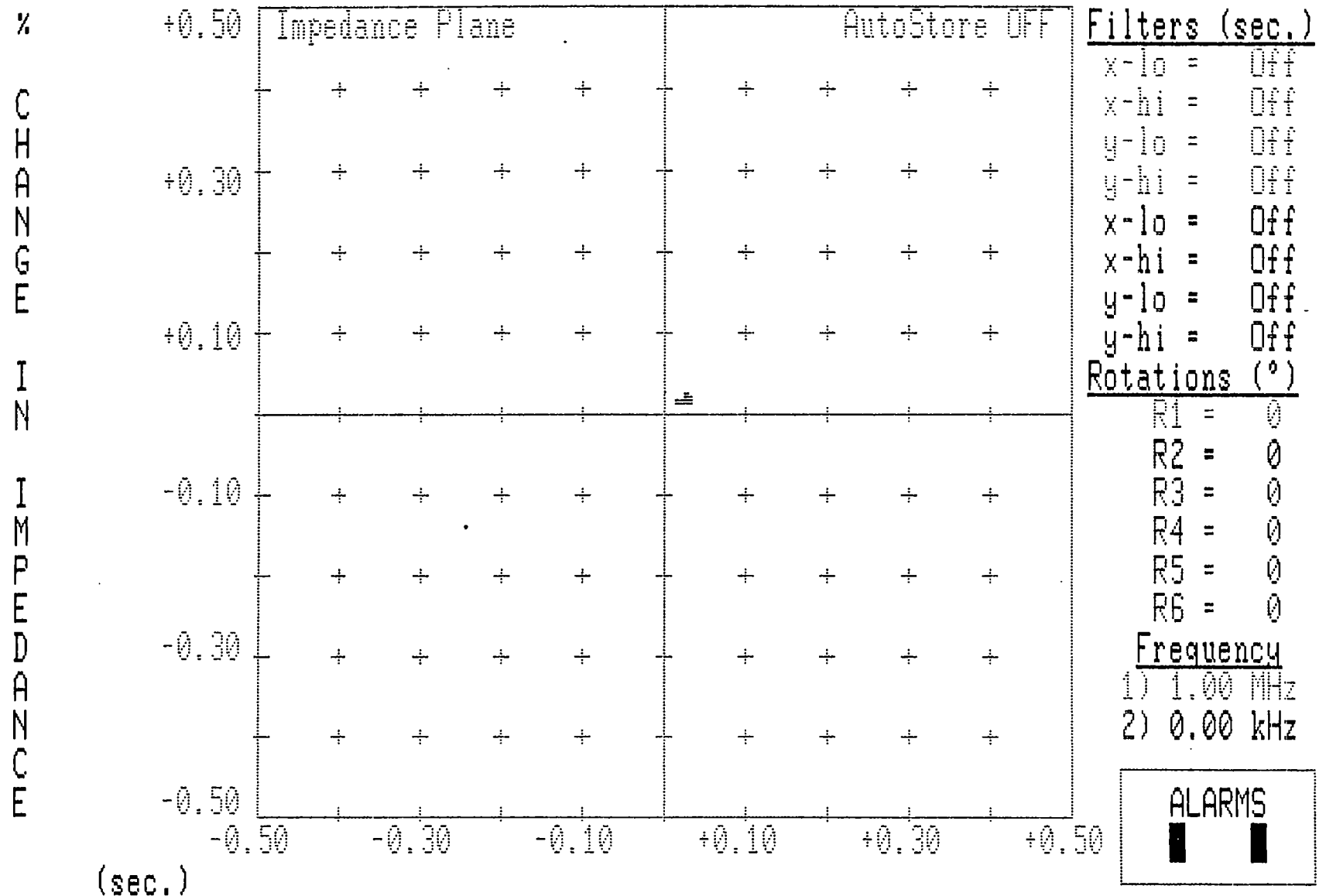




HOME replay SHIFT-HOME exit SPACEBAR alrm reset ↑ norm speed SHIFT-↑ erase  
 ↓ slow motion SHIFT-↓ ultra slow motion + start flag → end flag

10 mm DIAMETER TEST COIL WITH COPPER WINDING  
 IMPEDANCE CHANGE FOR A 70°C TEMPERATURE DEPRESSION

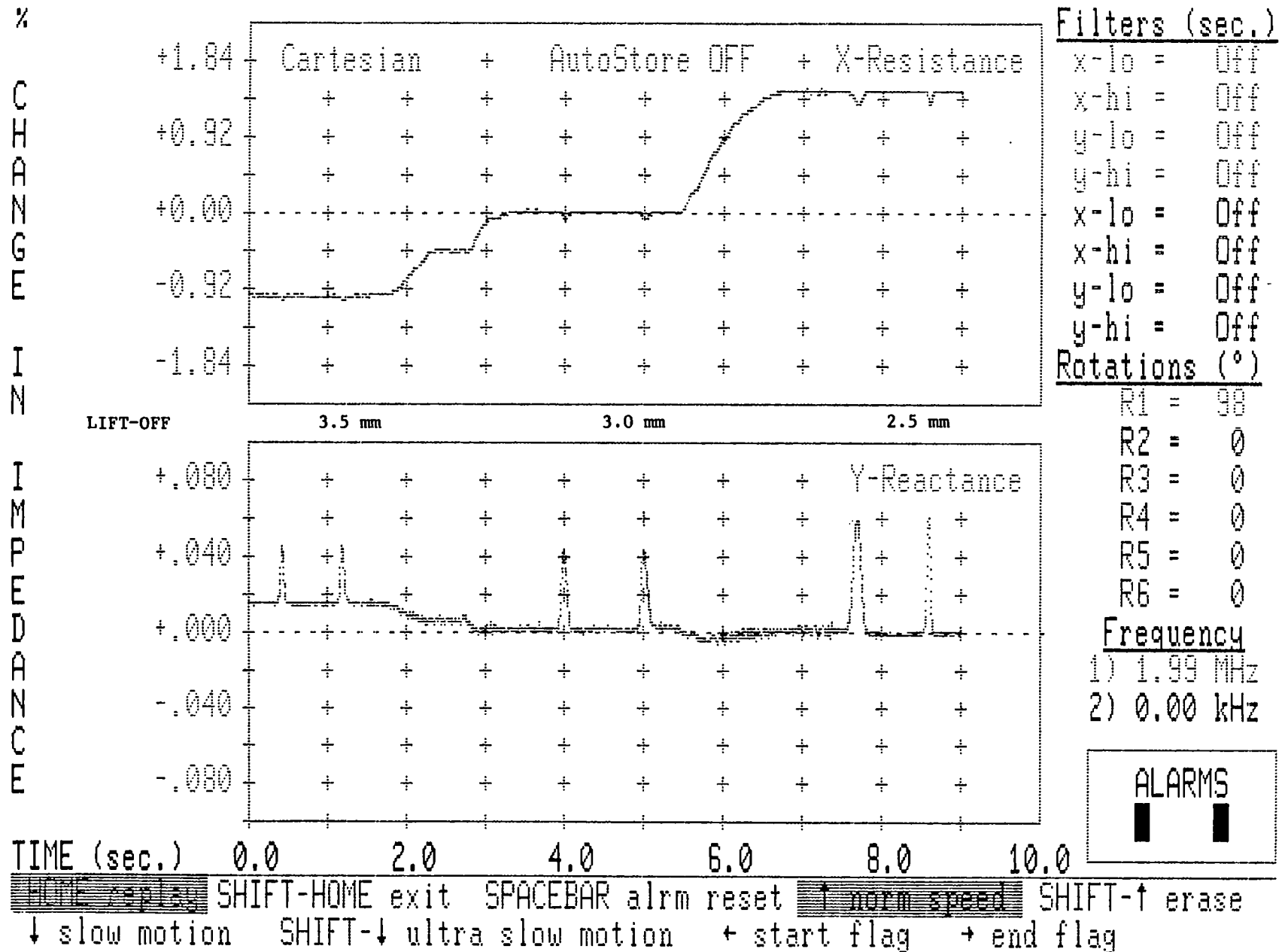
FIG. 1



~~HOME reset~~ SHIFT-HOME exit SPACEBAR alrm reset ~~f norm speed~~ SHIFT-f erase  
↓ slow motion SHIFT-↓ ultra slow motion + start flag → end flag

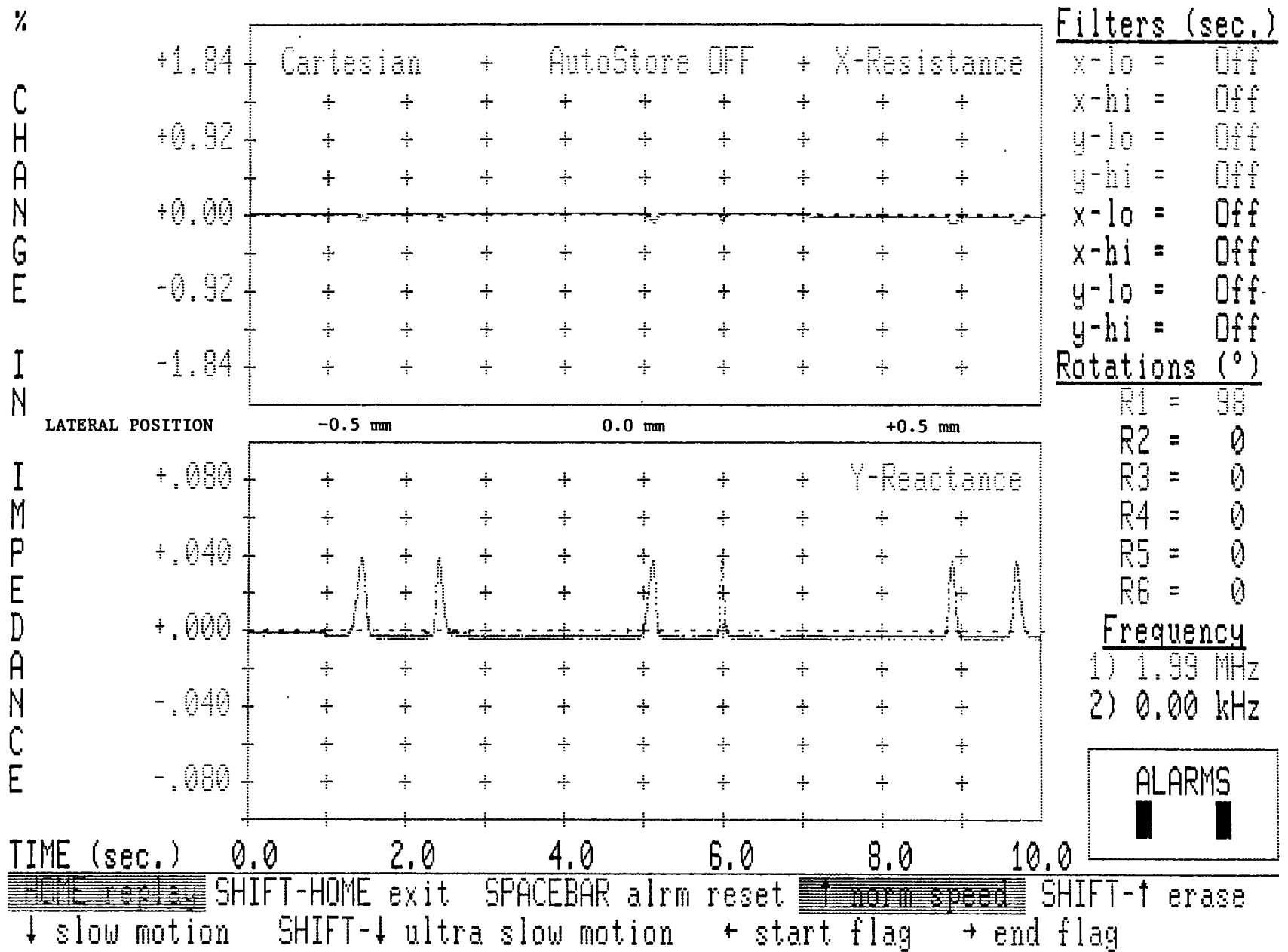
10 mm DIAMETER TEST COIL WITH CONSTANTAN WINDING  
IMPEDANCE CHANGE FOR A 70°C TEMPERATURE DEPRESSION

FIG. 2



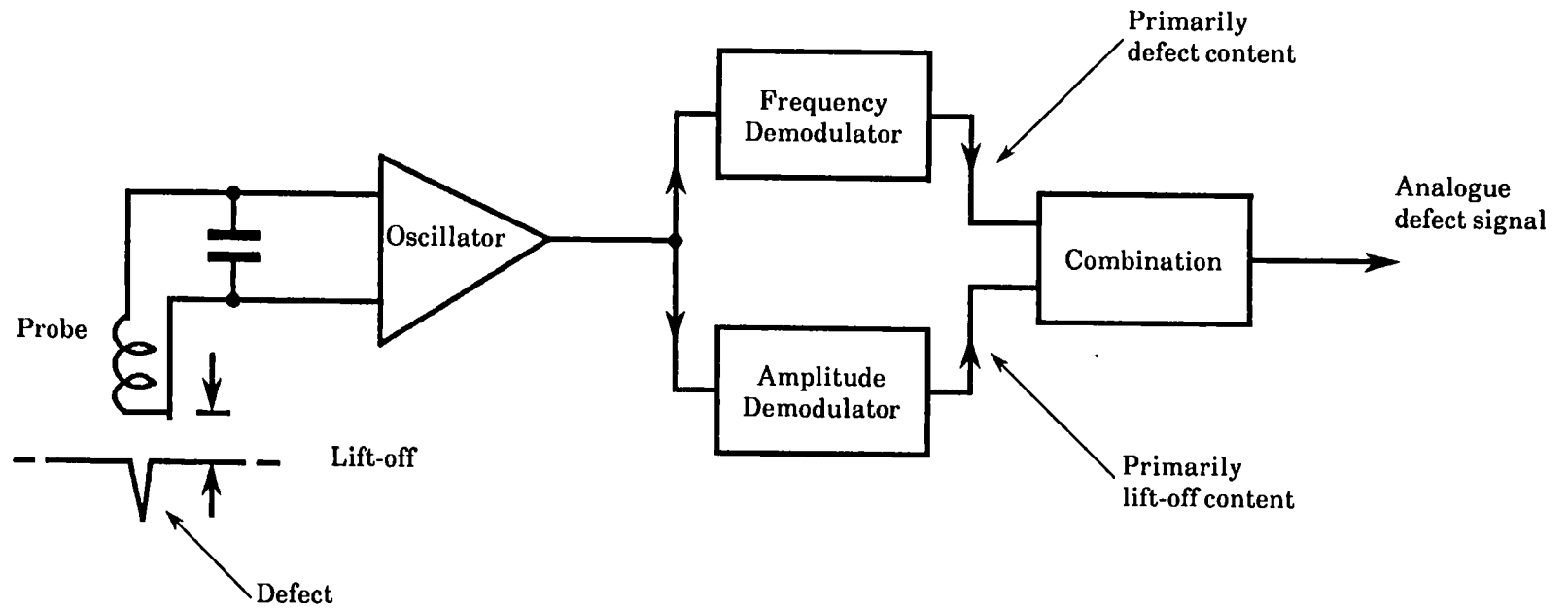
SINGLE 10 mm DIAMETER TEST COIL  
 1 mm DEFECT IN TITANIUM ALLOY BAR  
 (SHOWING VERTICAL MOVEMENT)

FIG. 3



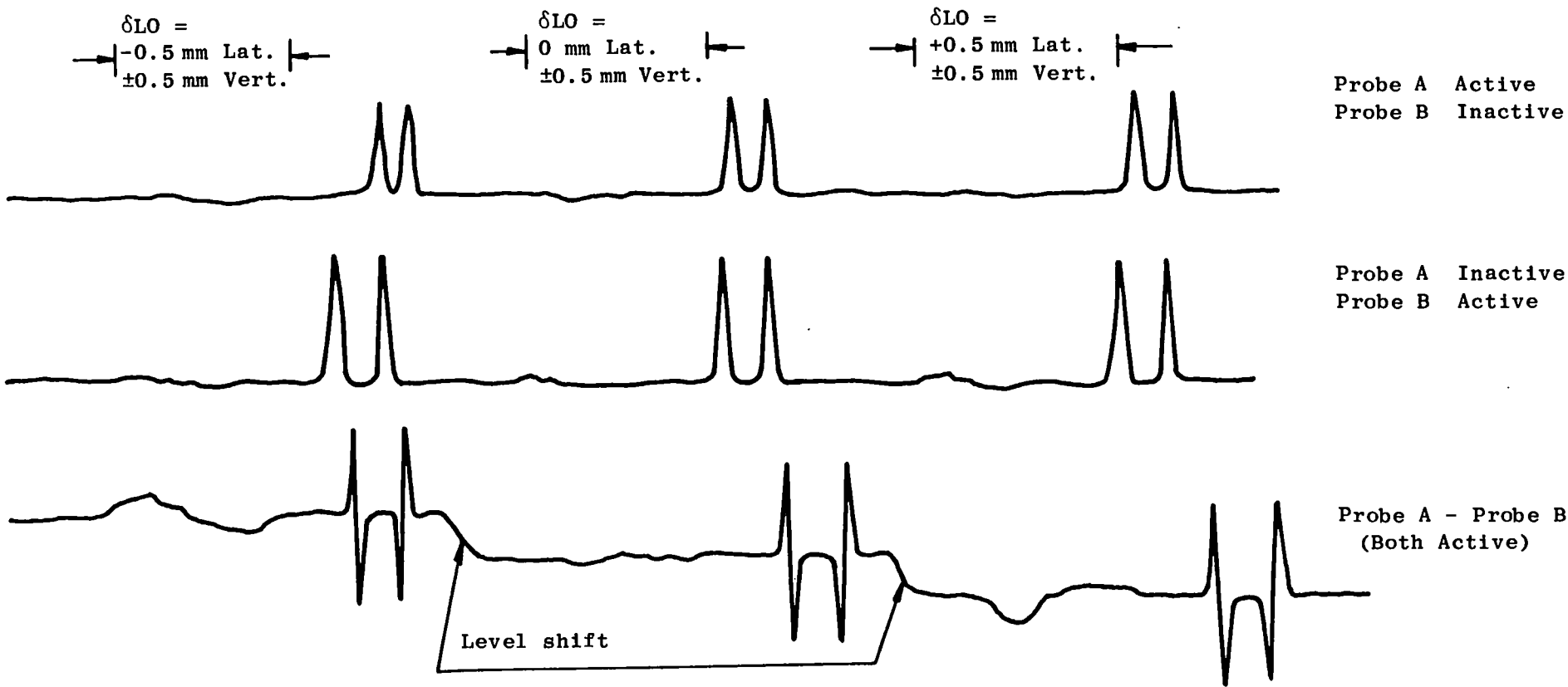
**SINGLE 10 mm DIAMETER TEST COIL  
 1 mm DEFECT IN TITANIUM ALLOY BAR  
 (SHOWING LATERAL MOVEMENT)**

**FIG. 4**



BLOCK DIAGRAM OF RESONANT PROBE CONCEPT

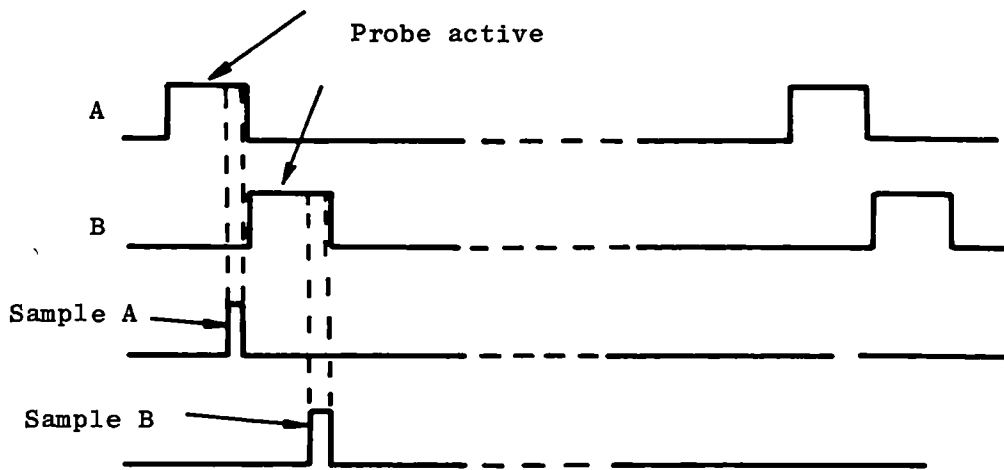
FIG. 5



All defects = 1 mm  
Nominal Lift-off = 3.5 mm

INTERACTION OF ADJACENT PROBES SUBJECT TO VERTICAL AND LATERAL LIFT-OFF

FIG. 6 (R3/6160)



**PROBE COMMUTATION SAMPLING SEQUENCE**  
 (NOT EMPLOYED IN FINAL DESIGN)

**FIG. 7**  
**(R3/6161)**

Nominal Lift-off = 3.5 mm

Commutation Frequency = 1 kHz

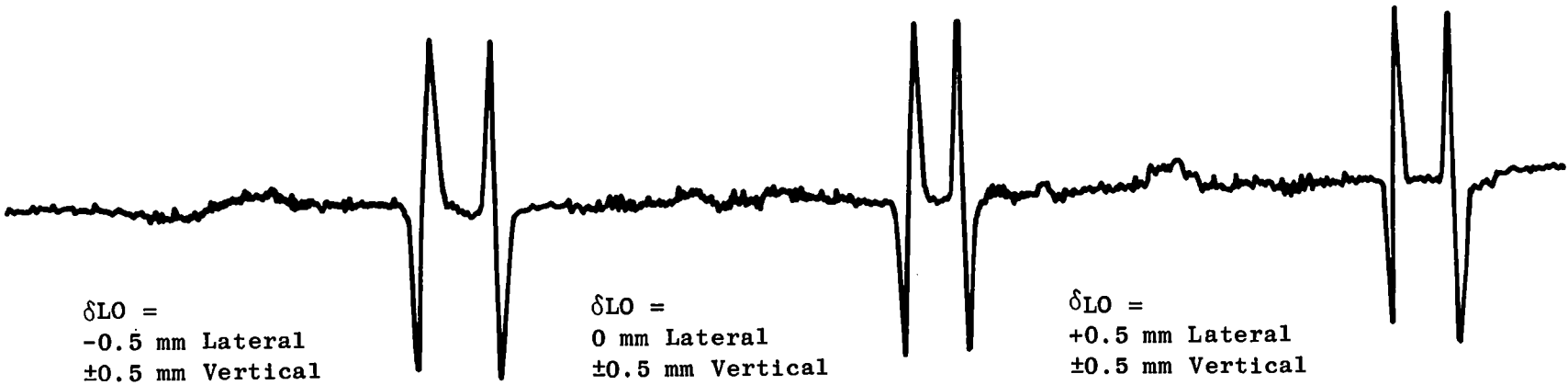
Probe A



Probe B



20



$\delta LO =$   
-0.5 mm Lateral  
 $\pm 0.5$  mm Vertical

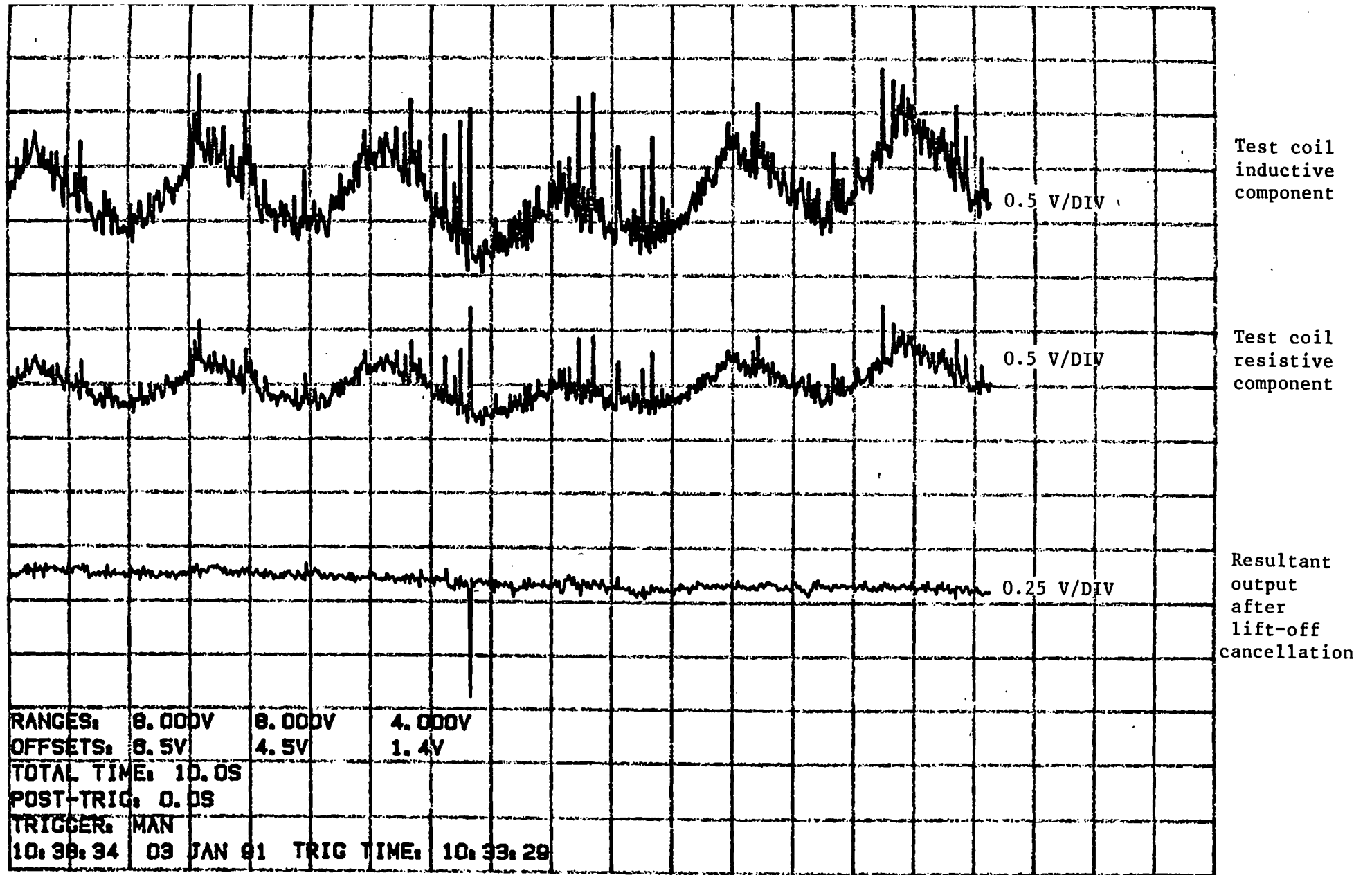
$\delta LO =$   
0 mm Lateral  
 $\pm 0.5$  mm Vertical

$\delta LO =$   
+0.5 mm Lateral  
 $\pm 0.5$  mm Vertical

2 PROBE COMMUTATION SYSTEM

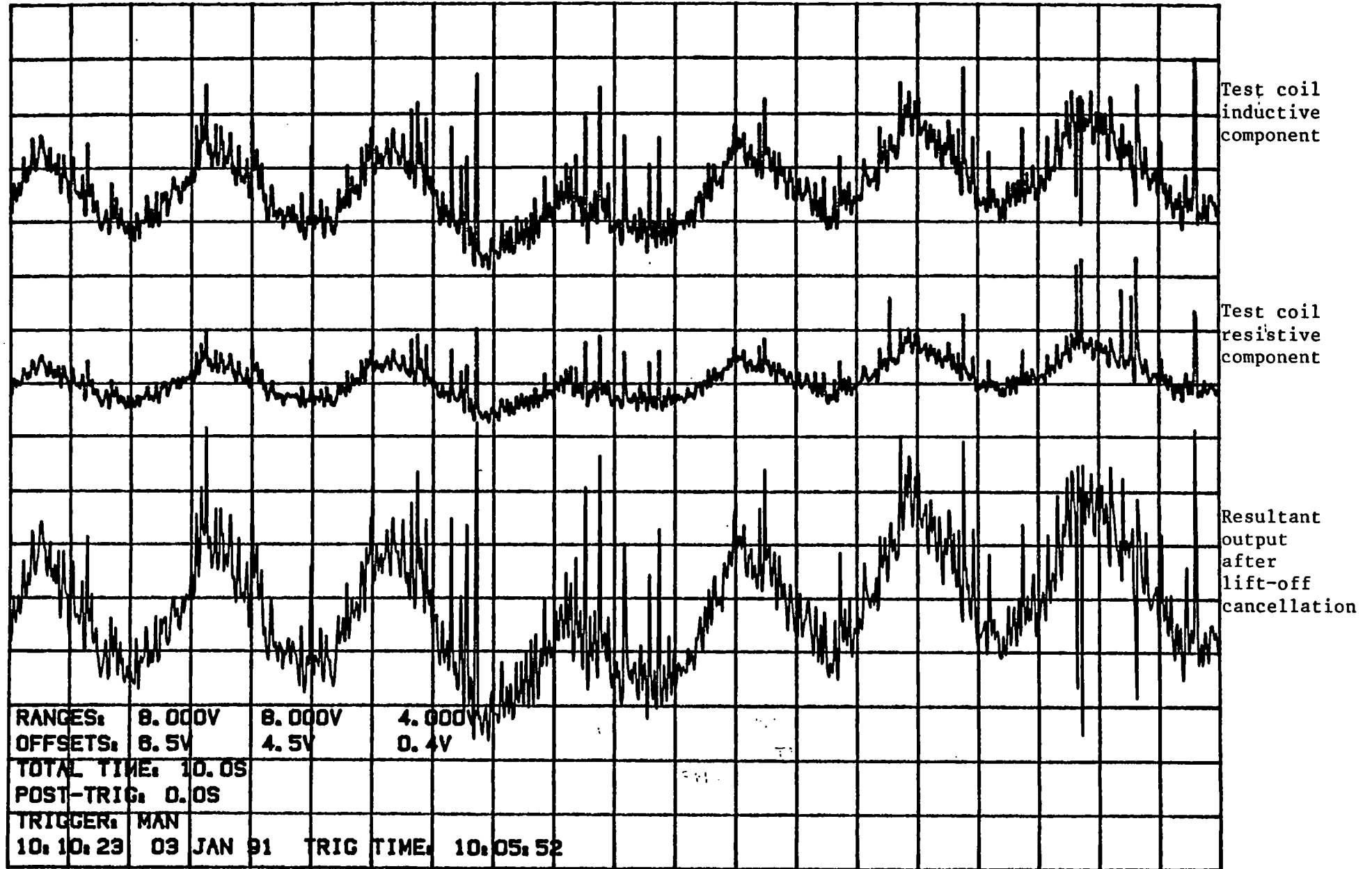
FIG. 8  
(R3/6162)





HOT BAR INSPECTION SIGNALS USING CANCELLATION FACTOR BASED ON HOT STEEL BAR

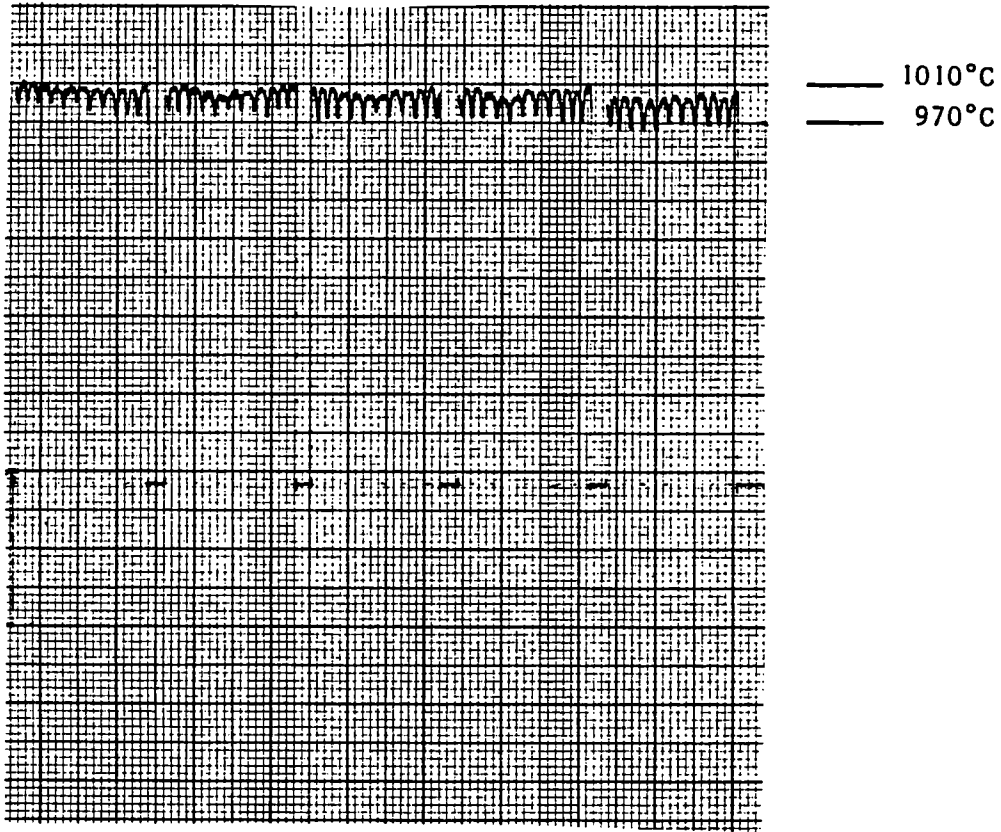
FIG. 9



HOT BAR INSPECTION SIGNALS USING CANCELLATION FACTOR BASED ON  
TITANIUM ALLOY BAR

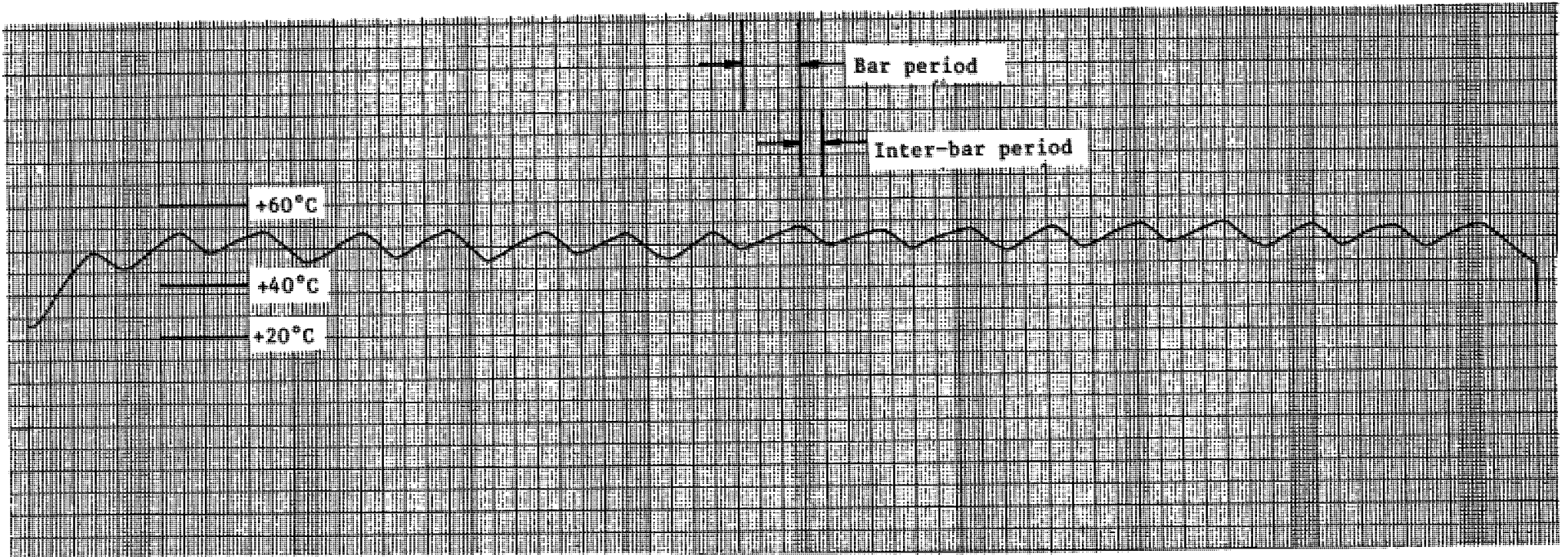
FIG. 10

←————→ Bar period



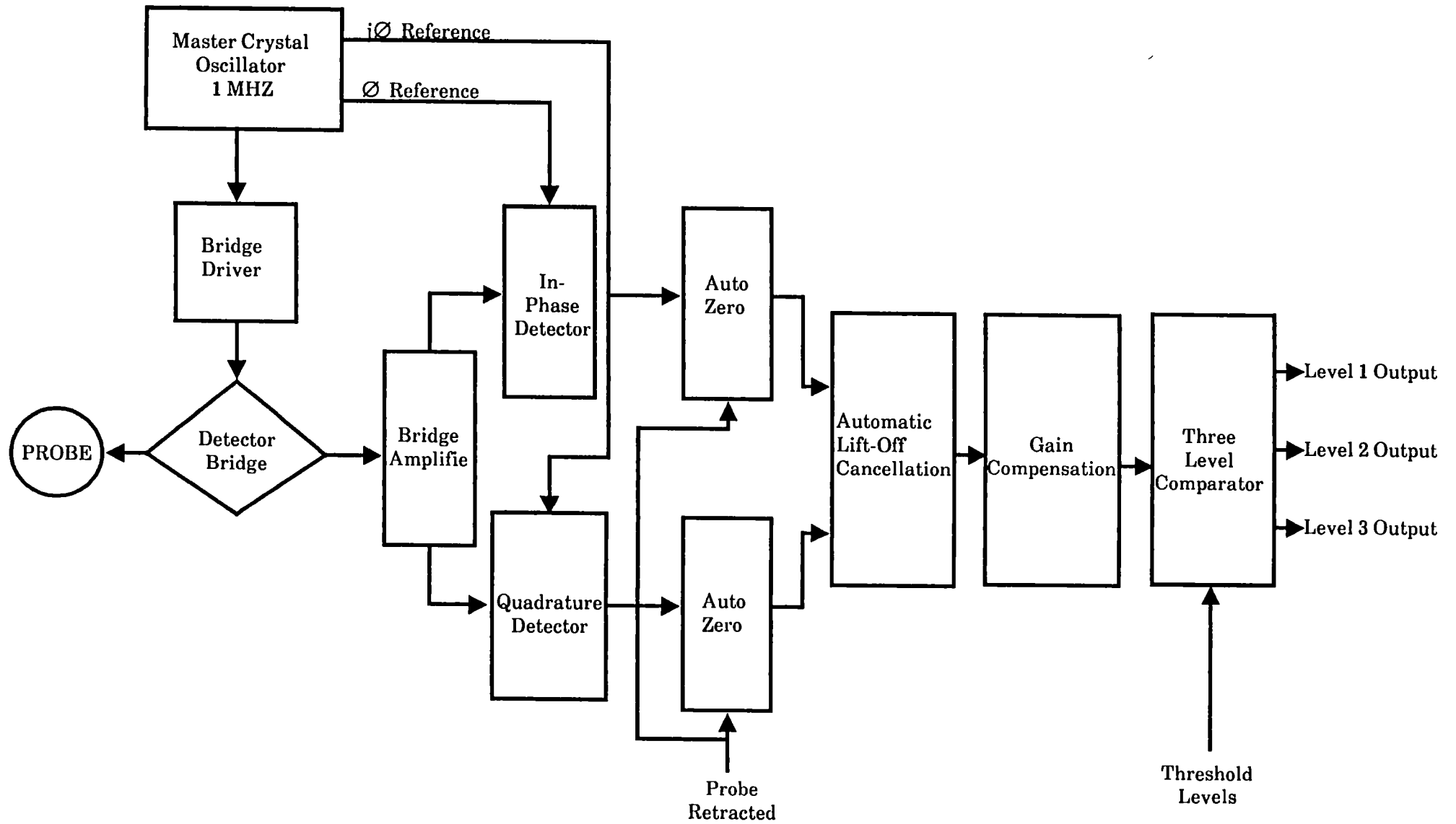
**BAR TEMPERATURE PROFILES DURING HOT BAR TRIALS**

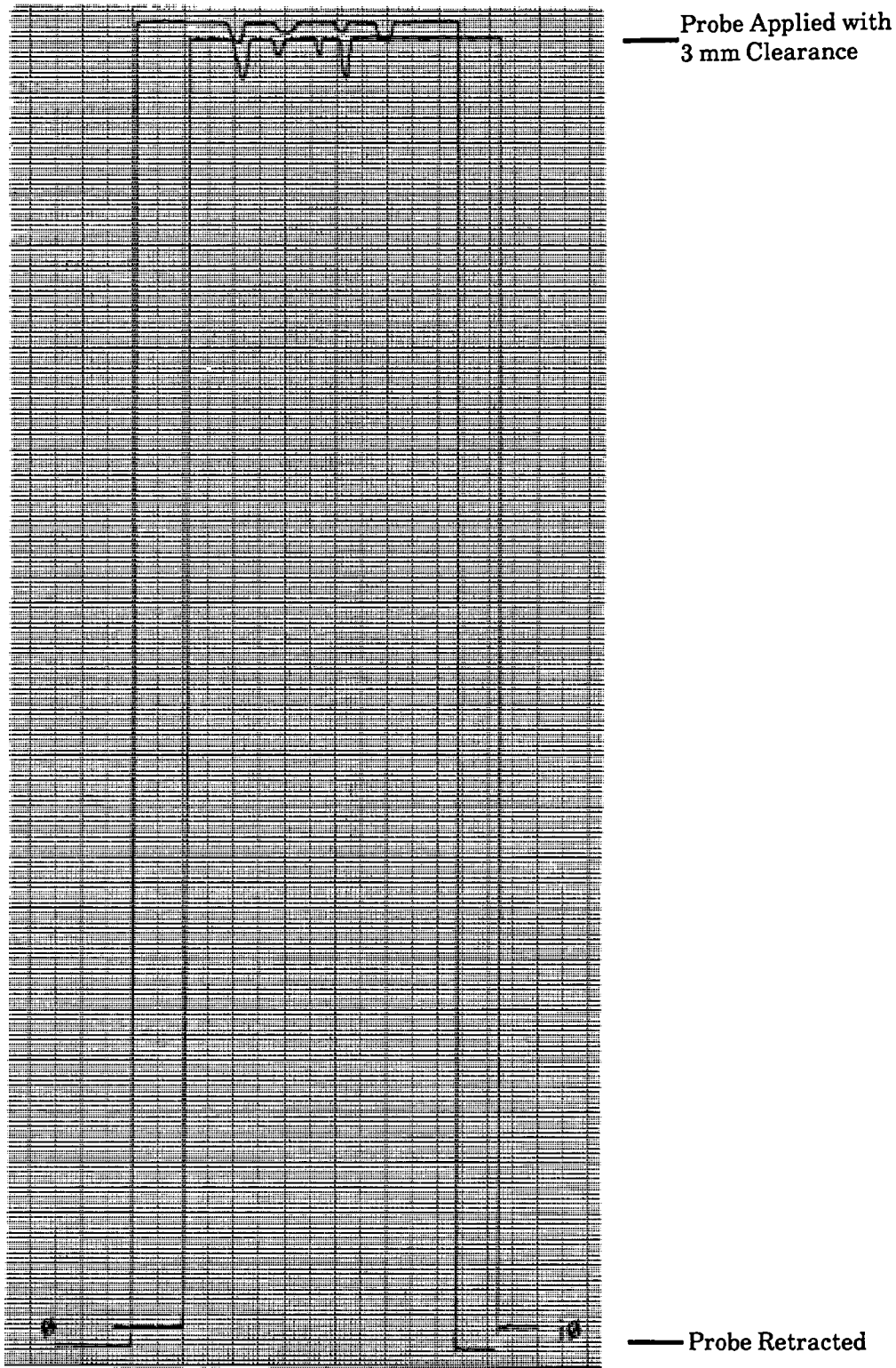
**FIG. 11**



VARIATIONS IN TEST COIL TEMPERATURE DURING HOT BAR TRIALS

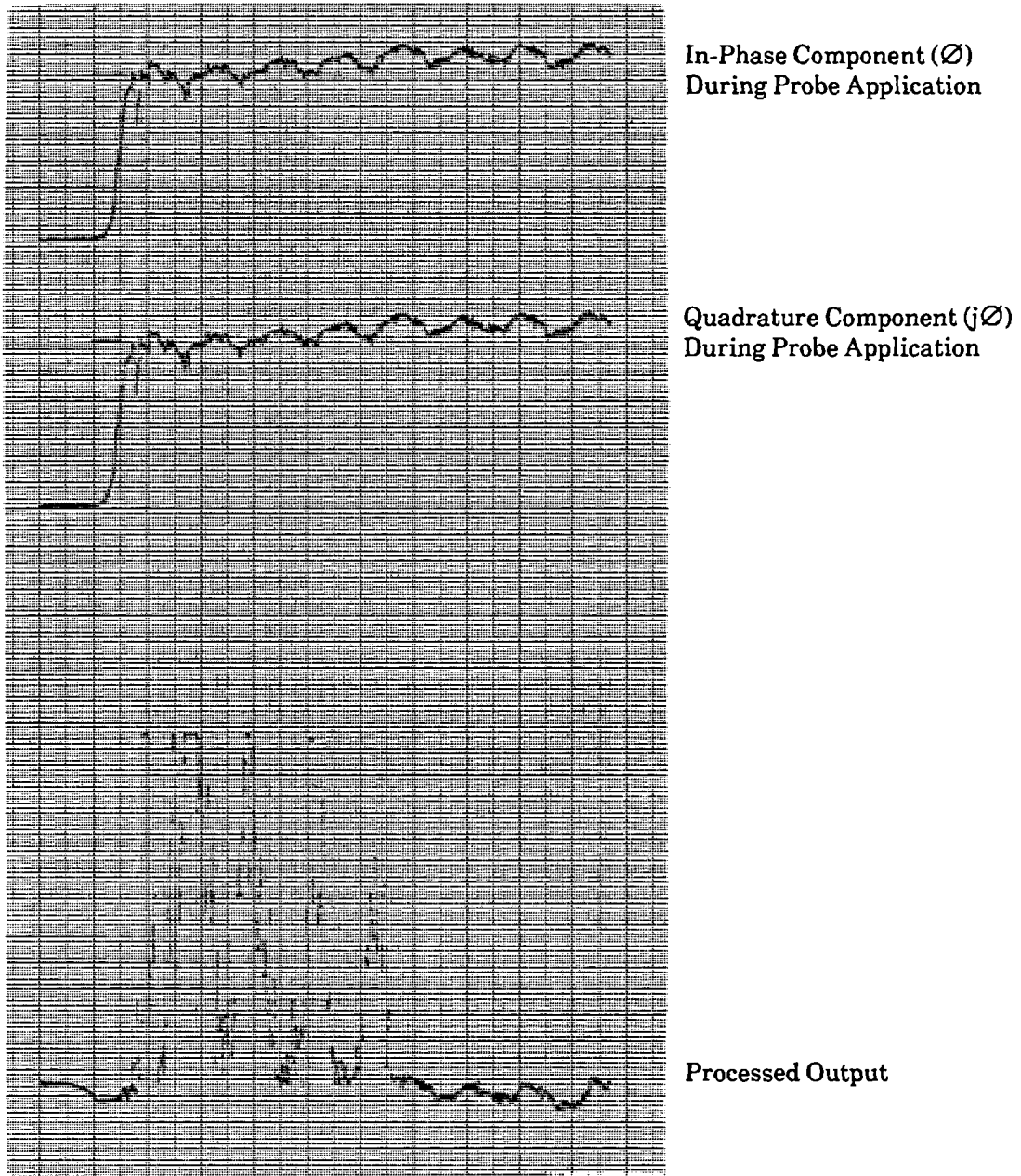
FIG. 12





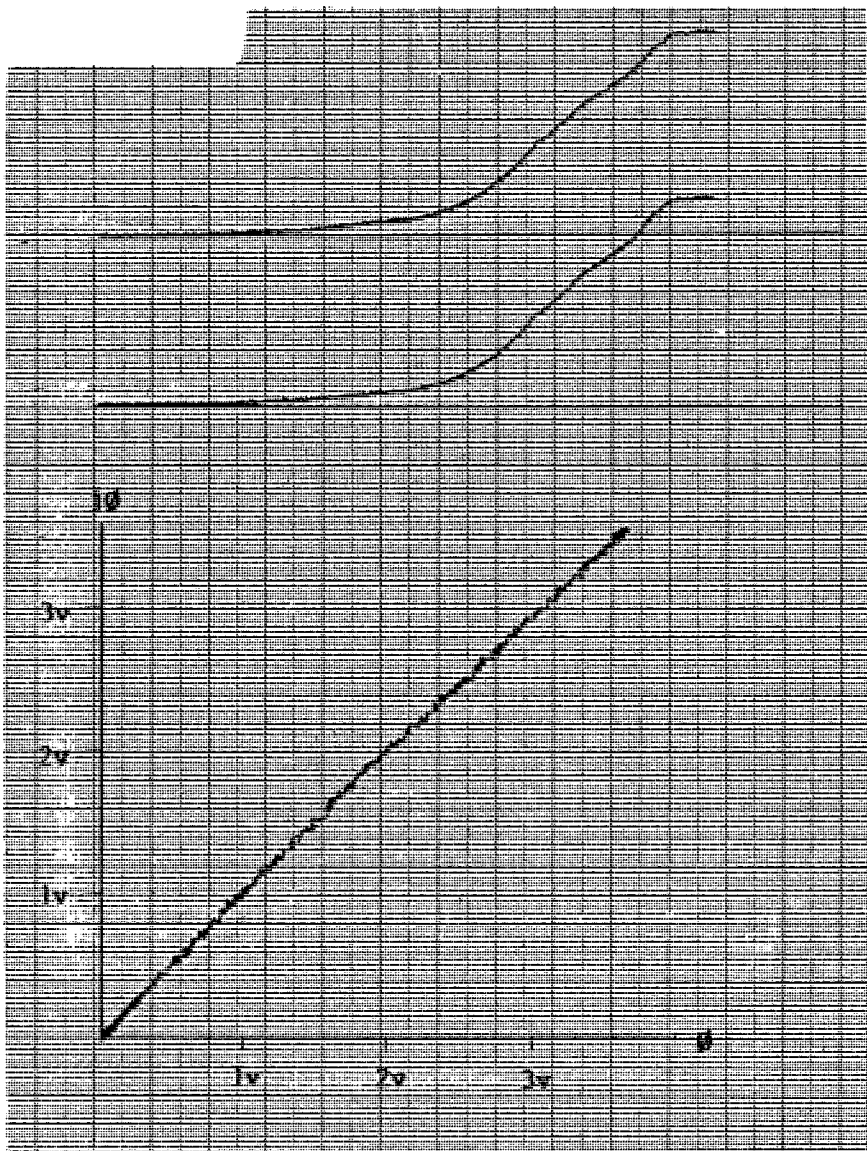
**RELATIONSHIP BETWEEN VOLTAGE CHANGE DURING PROBE APPLICATION AND VOLTAGE CHANGE FOR A 0.5 mm AND 1.0 mm DEFECT**

**FIG. 14**



**PROCESSED DEFECT OUTPUT WITH DELAYED  
LIFT-OFF CANCELLATION**

**FIG. 15**



Quadrature Component ( $j\varnothing$ )  
During Probe Application

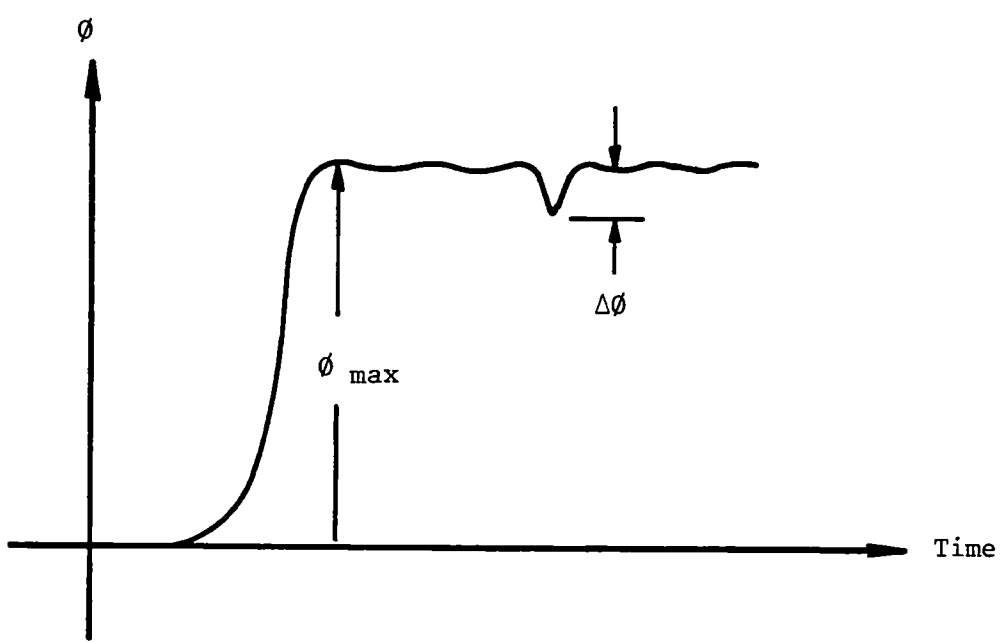
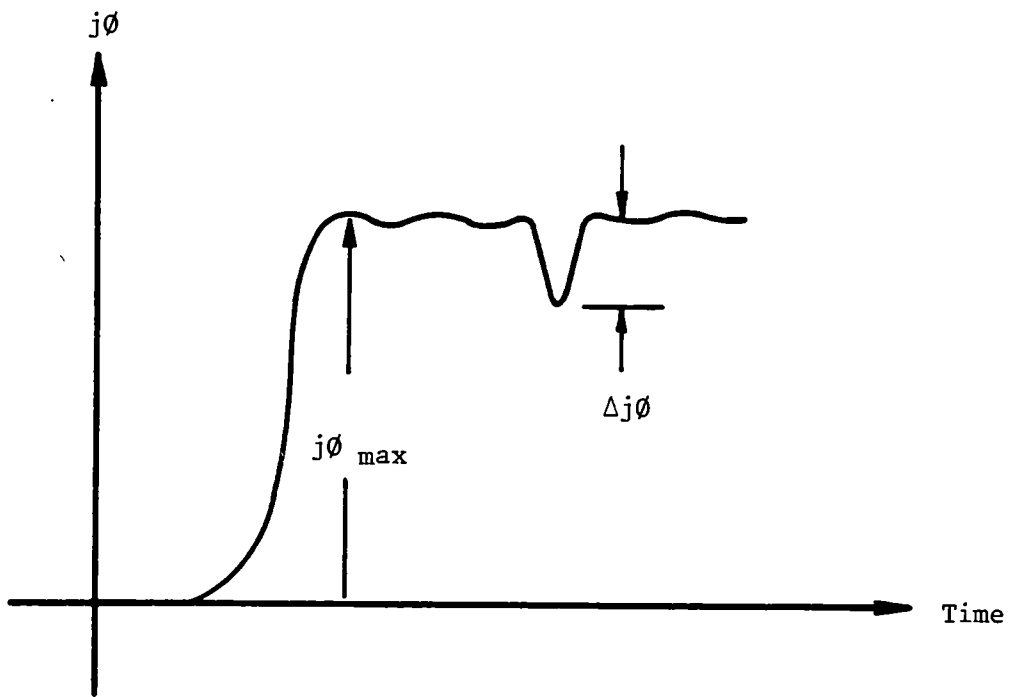
In-Phase Component ( $\varnothing$ )  
During Probe Application

Plot of  $\varnothing$  versus  $j\varnothing$

**RELATIONSHIP BETWEEN IN-PHASE AND QUADRATURE  
COMPONENTS DURING PROBE APPLICATION**

**FIG. 16**

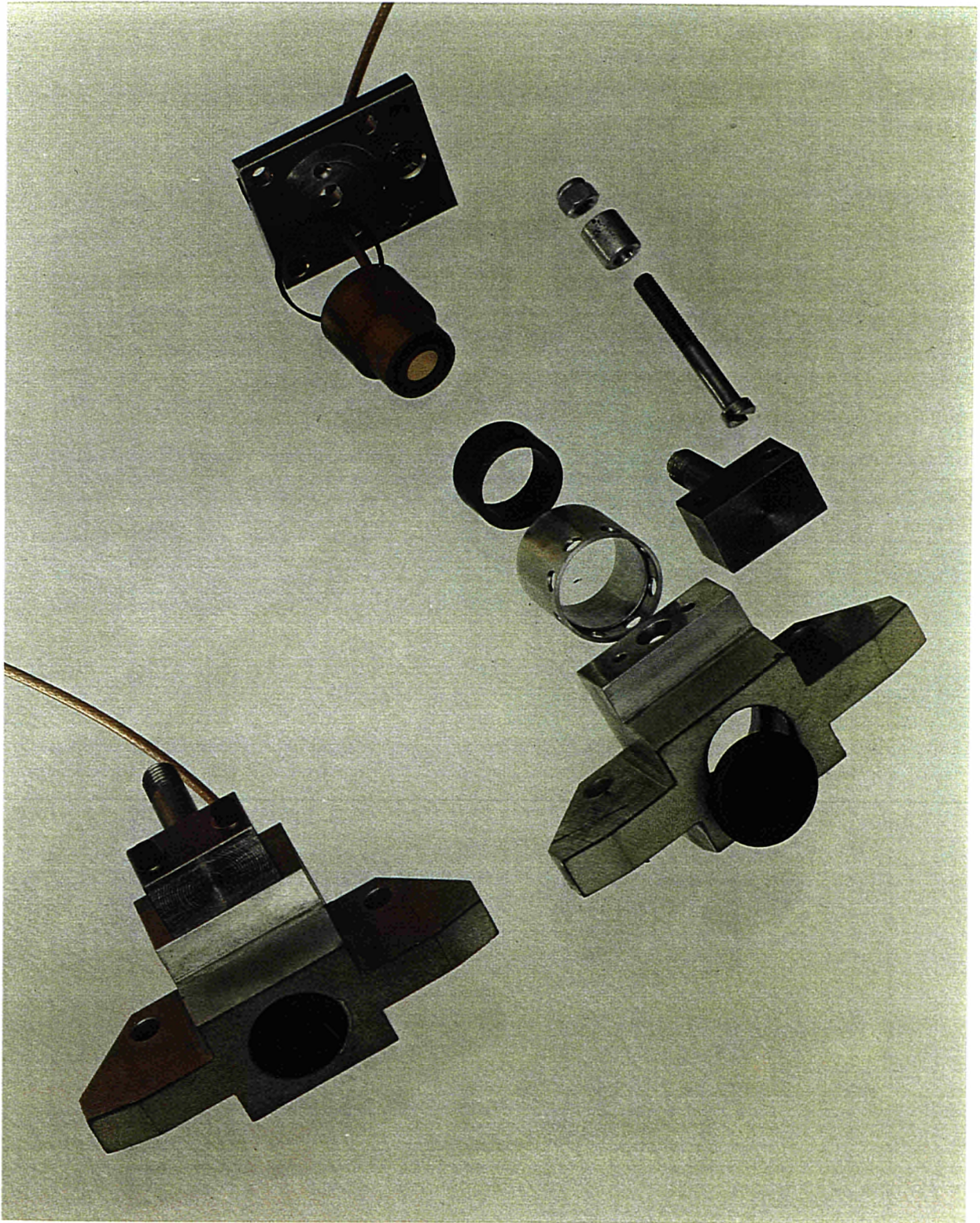




DEFINITION OF TERMS USED IN LIFT-OFF CANCELLATION

FIG. 17  
(R3/8404)

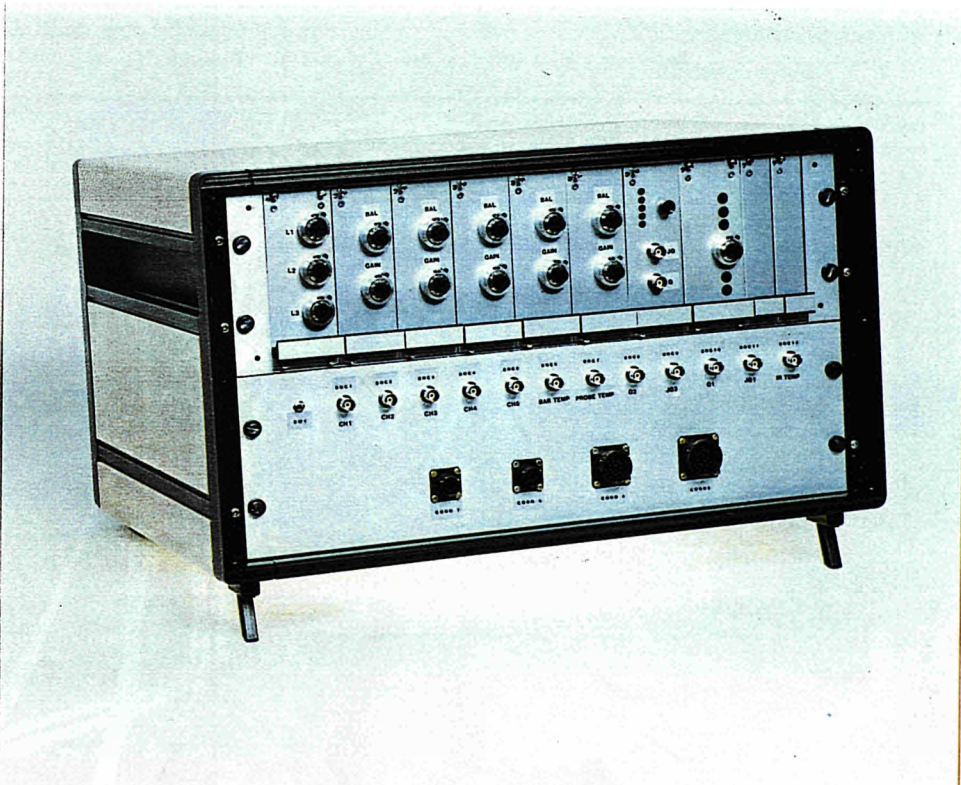
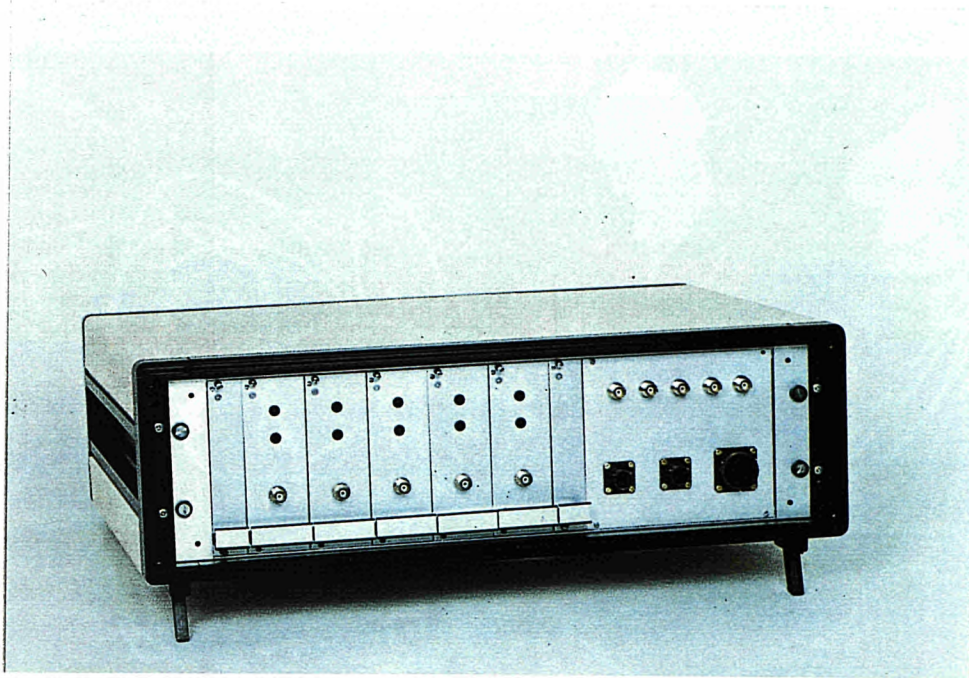




**EXPLODED VIEW OF INSPECTION COIL ASSEMBLY**

**FIG. 18**

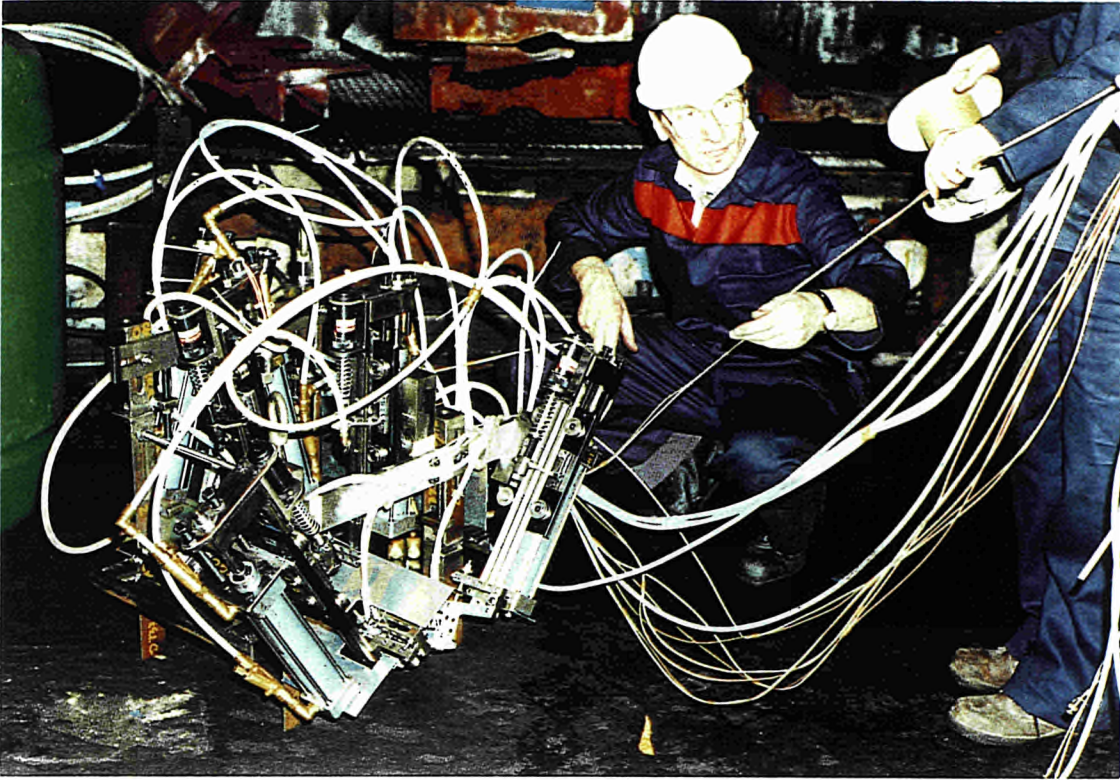




LOCAL AND REMOTE ELECTRONIC SIGNAL PROCESSING UNITS

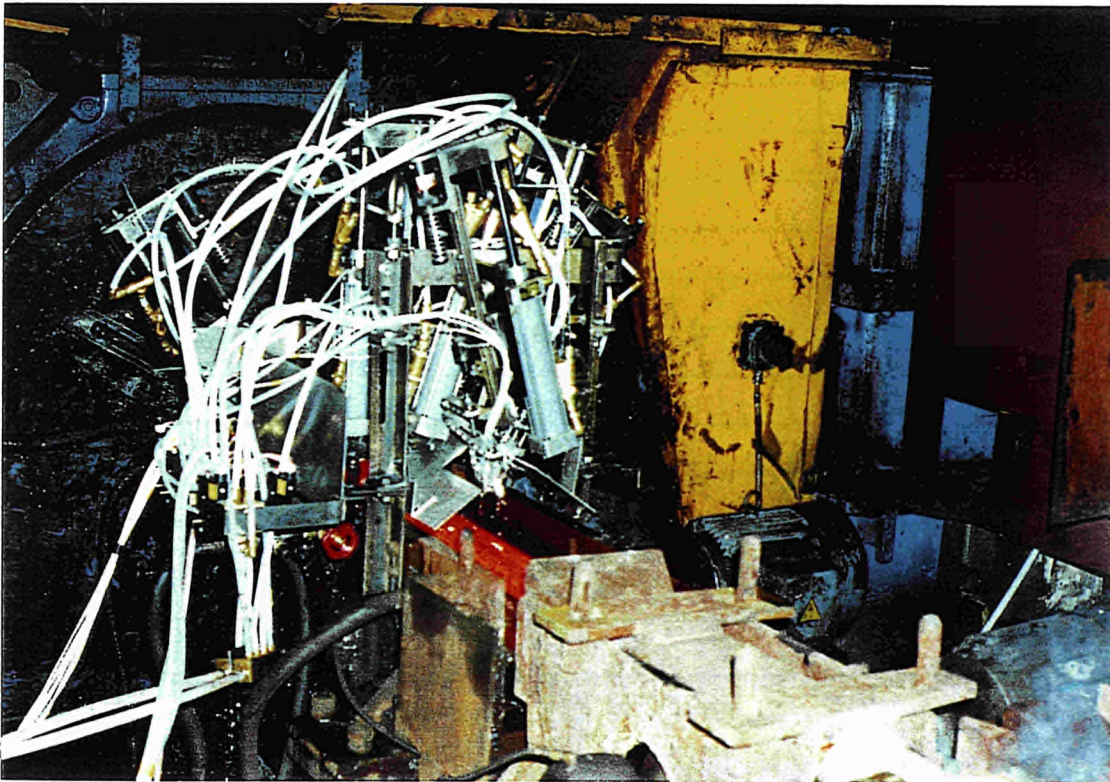
FIG. 19





**TEST HEAD ASSEMBLY DURING INSTALLATION**

**FIG. 20**



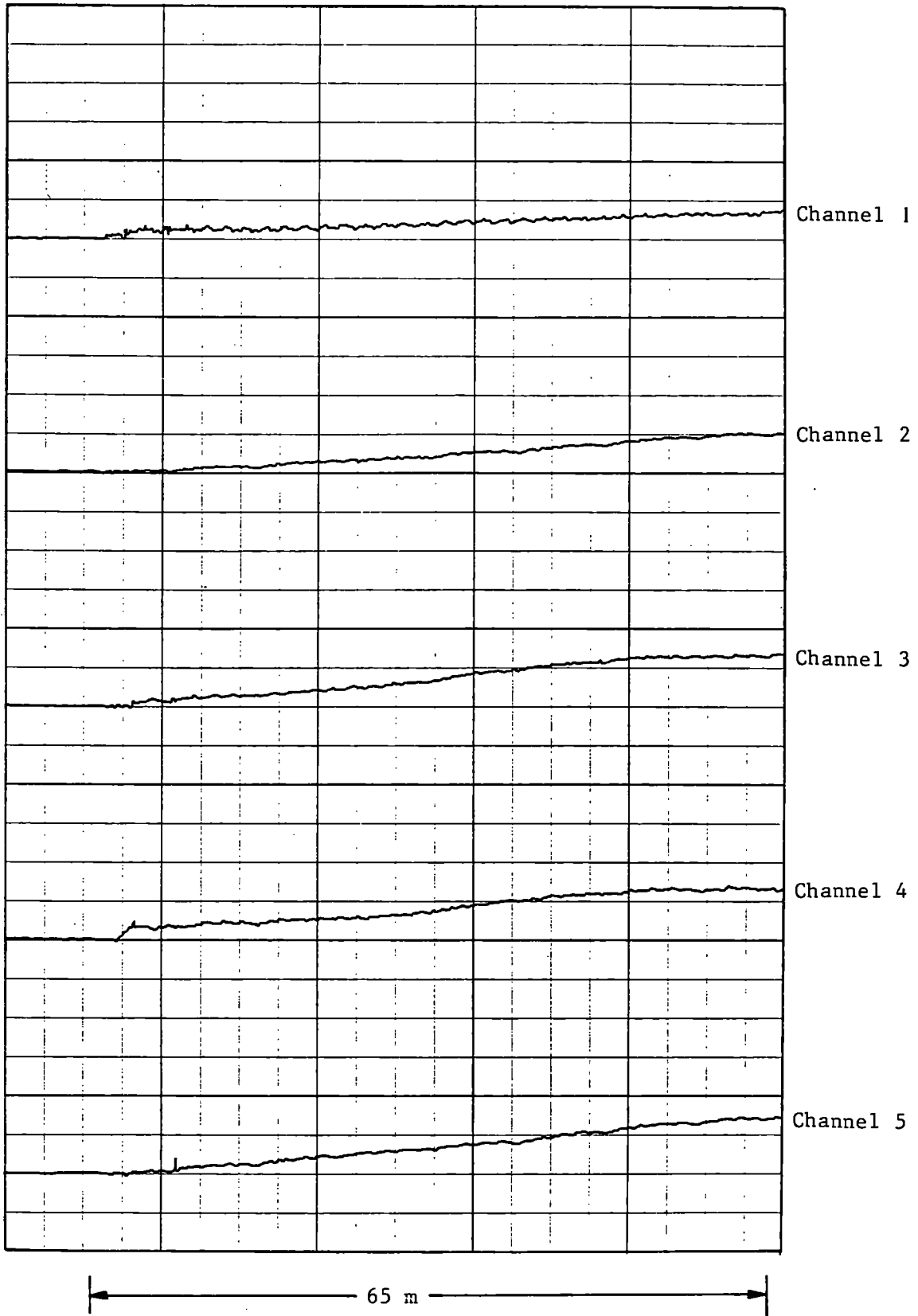
**TEST HEAD ASSEMBLY DURING PRODUCTION TRIALS**

**FIG. 21**





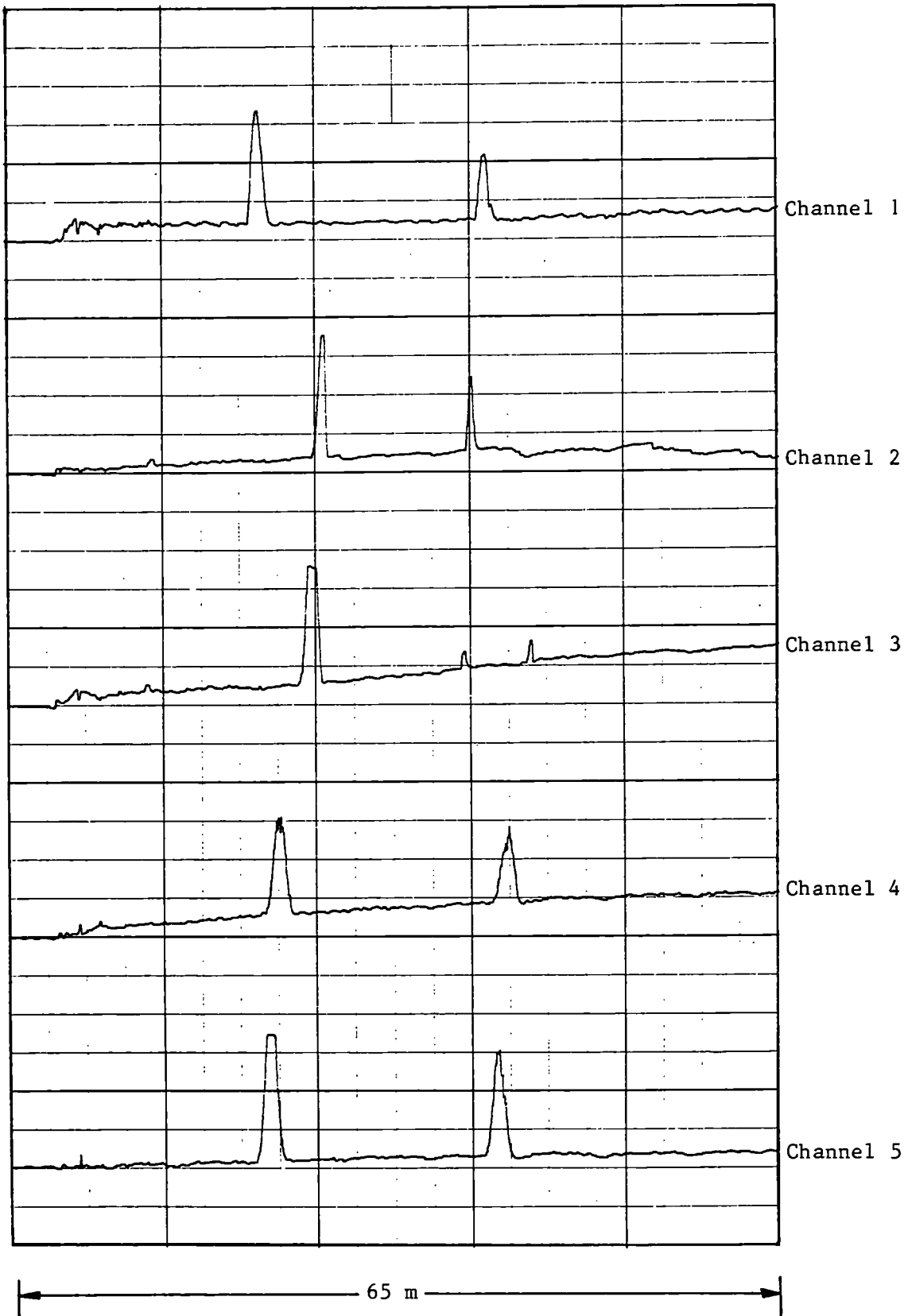
1 mm Calibration Defect  $\equiv$  2 Vertical Divisions



EDDY-CURRENT INSPECTION RESULTS FOR  
PRIME PRODUCTION BAR

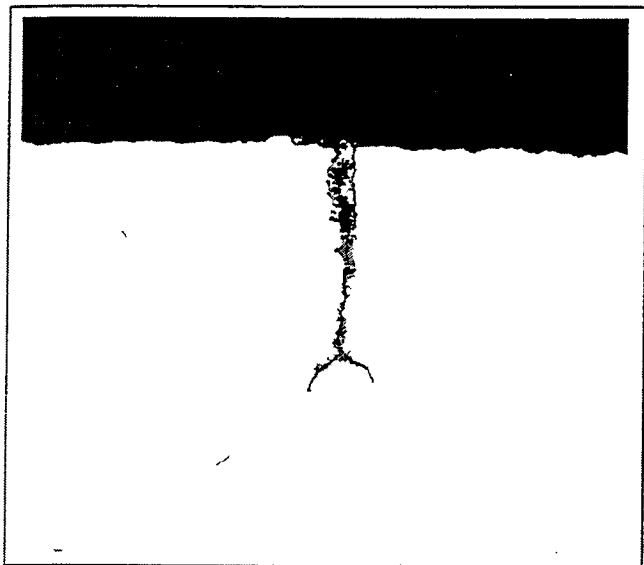
FIG. 22

1 mm Calibration Defect  $\equiv$  2 Vertical Divisions

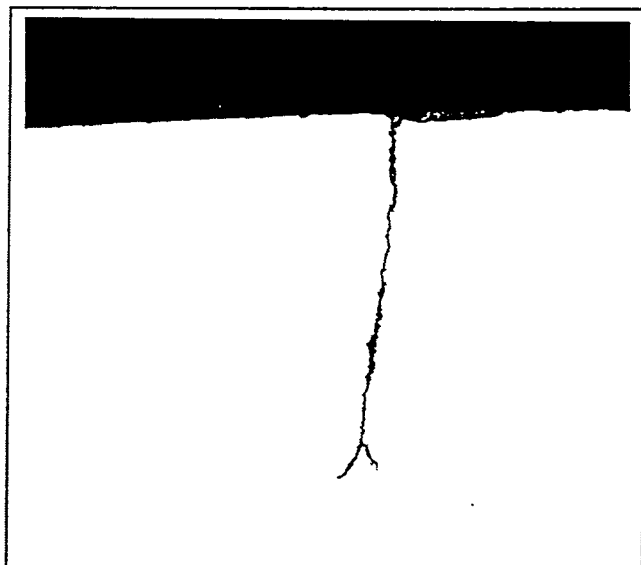


EDDY-CURRENT INSPECTION RESULTS FOR  
DEFECTIVE TRIAL BAR

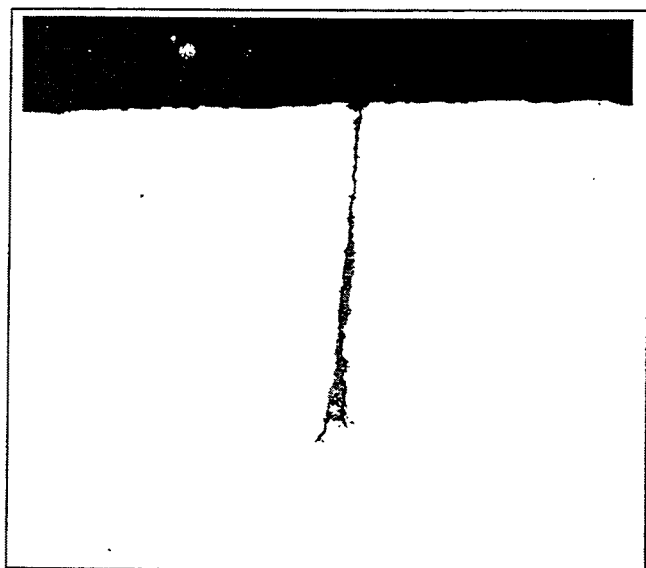
FIG. 23



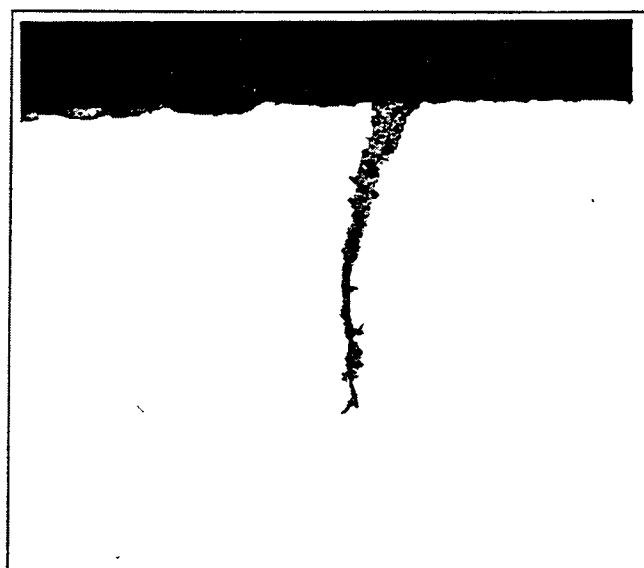
x 34



x 34



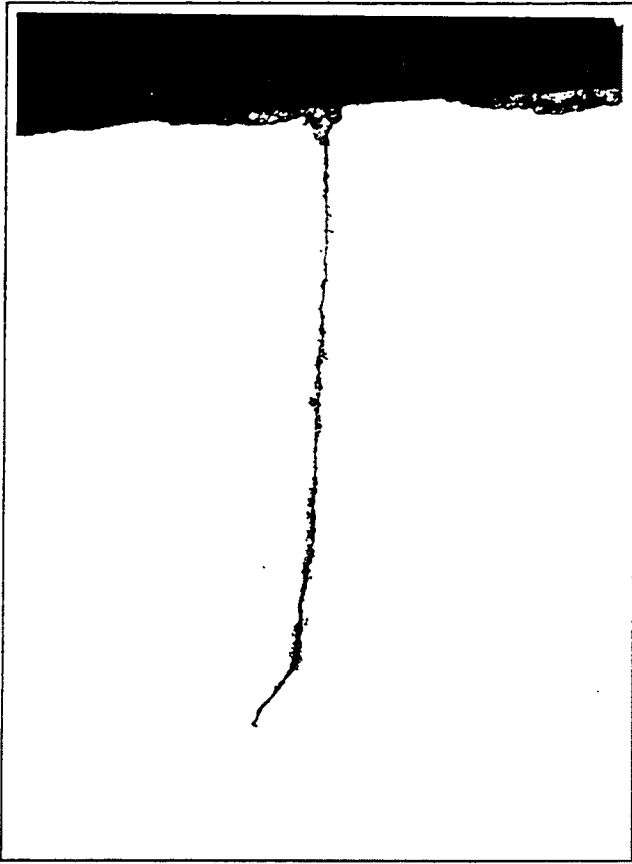
x 34



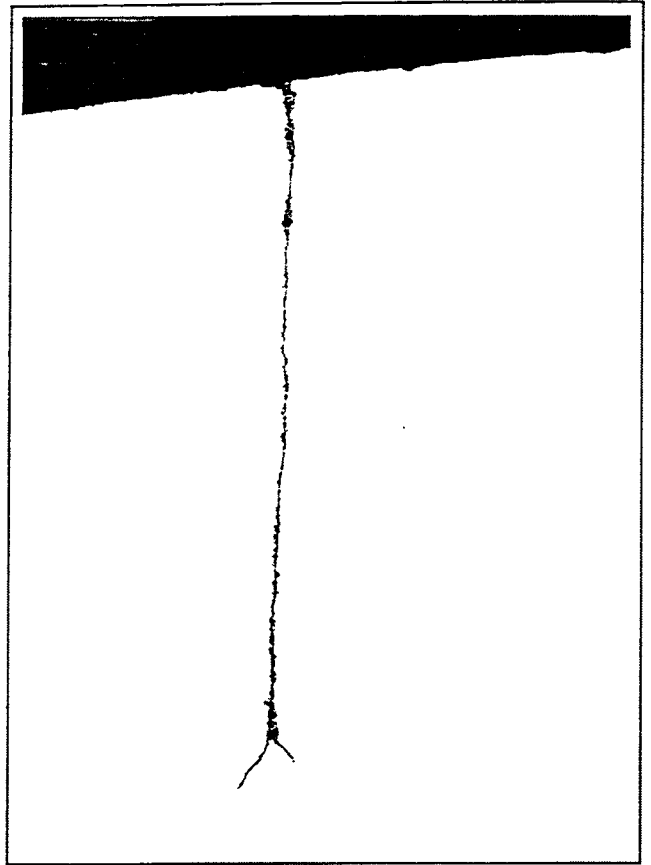
x 34

**TYPICAL MACROPHOTOGRAPHS OF THE  
NOMINAL 1.2 mm DEFECTIVE ZONE**

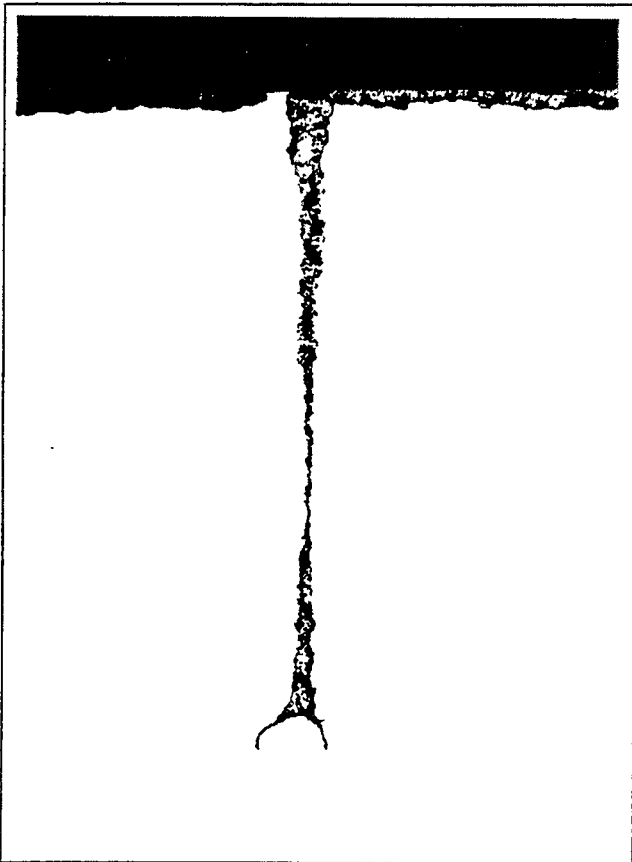
**FIG. 24**



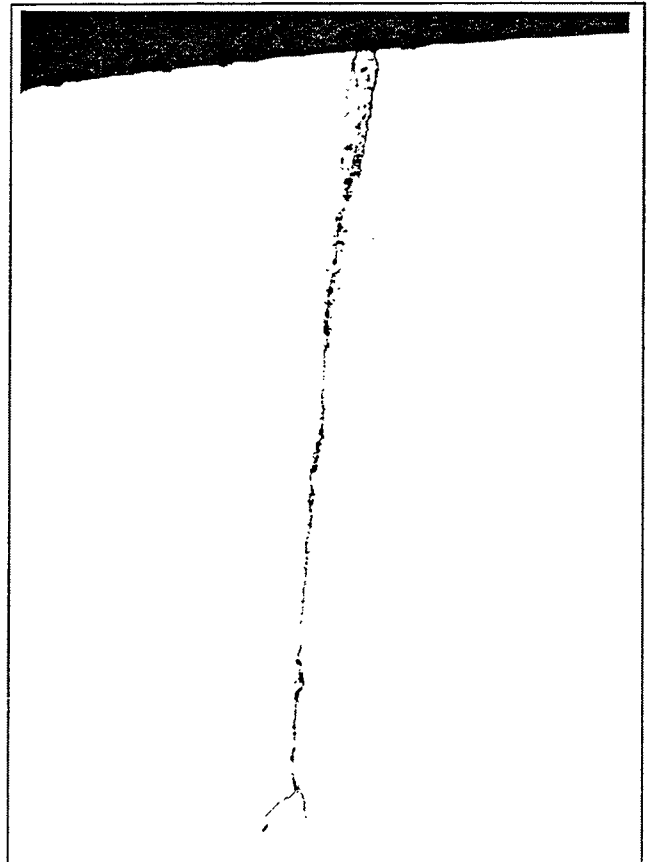
x 34



x 34



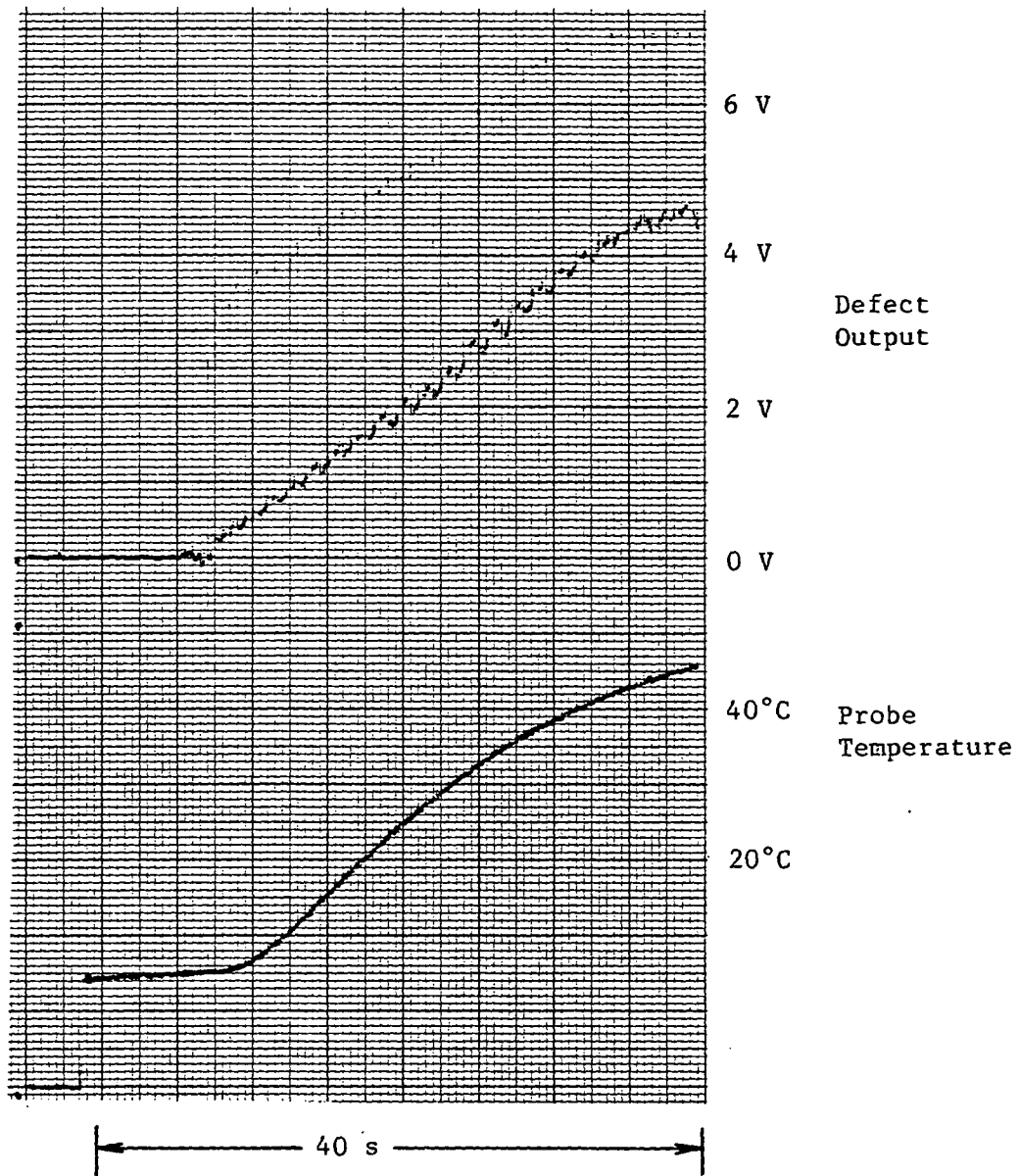
x 34



x 34

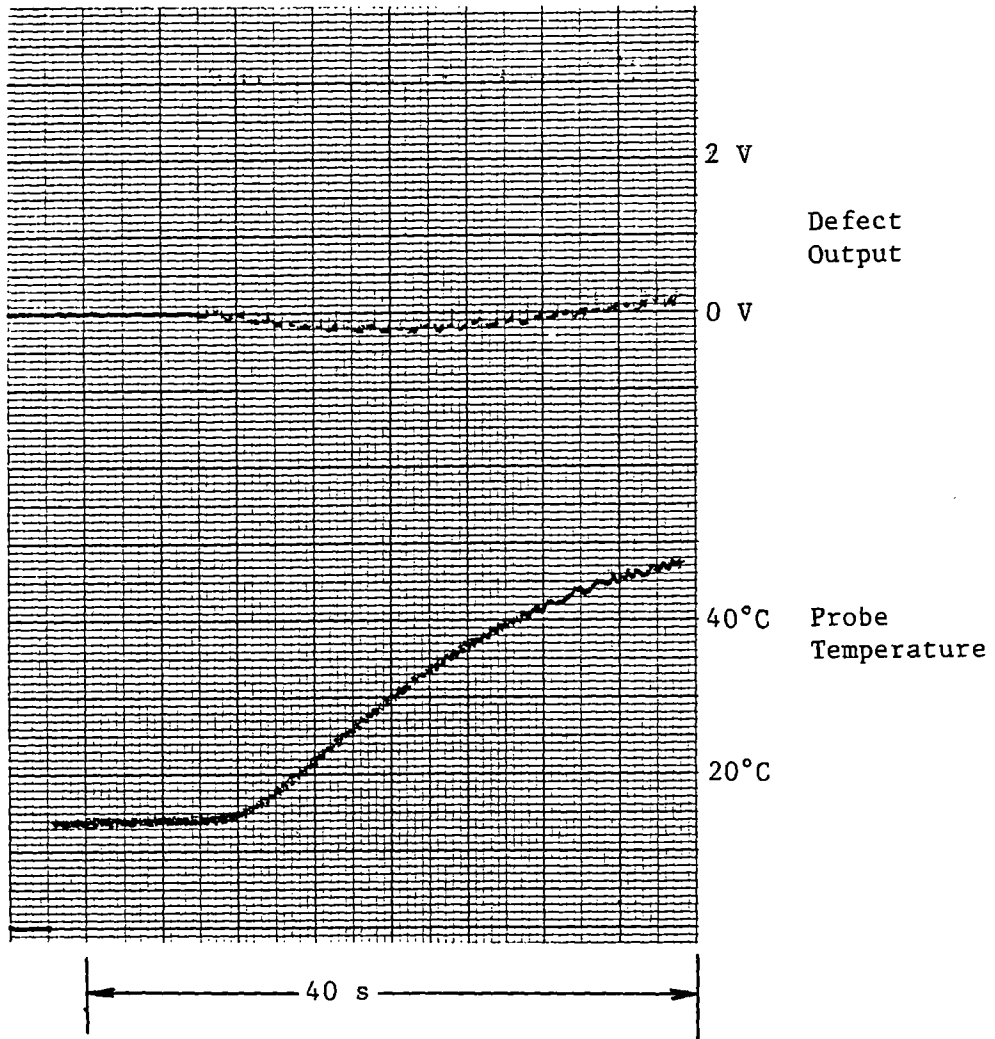
TYPICAL MACROPHOTOGRAPHS OF THE  
NOMINAL 2.4 mm DEFECTIVE ZONE

FIG. 25



PLOTS OF DEFECT OUTPUT AND PROBE TEMPERATURE  
 v TIME DURING REPEATED TRAVERSE OF THE  
 CALIBRATION NOTCH IN HOT STEEL WITH UNLAGGED LEADS

FIG. 26



**PLOTS OF DEFECT OUTPUT AND PROBE TEMPERATURE  
 v TIME DURING REPEATED TRAVERSE OF THE  
 CALIBRATION NOTCH IN HOT STEEL WITH LAGGED LEADS**

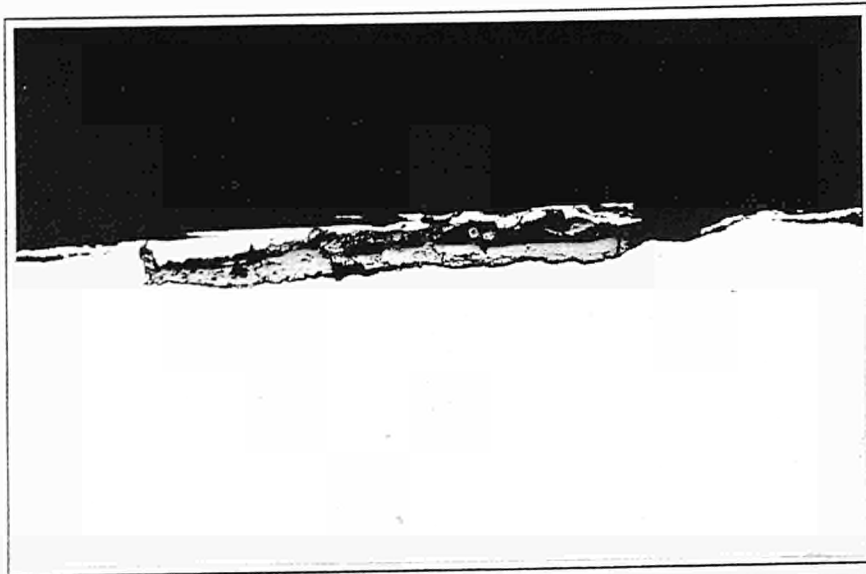
**FIG. 27**

N.B. Trace for Sample A shown at half scale



DEFECT RESPONSES FROM RESISTIVELY HEATED SAMPLES

FIG. 28



Sample A1

x 20



Sample A2

x 20



Sample A3

x 20

**MACROPHOTOGRAPHS OF RESISTIVELY HEATED  
DEFECT SAMPLES**

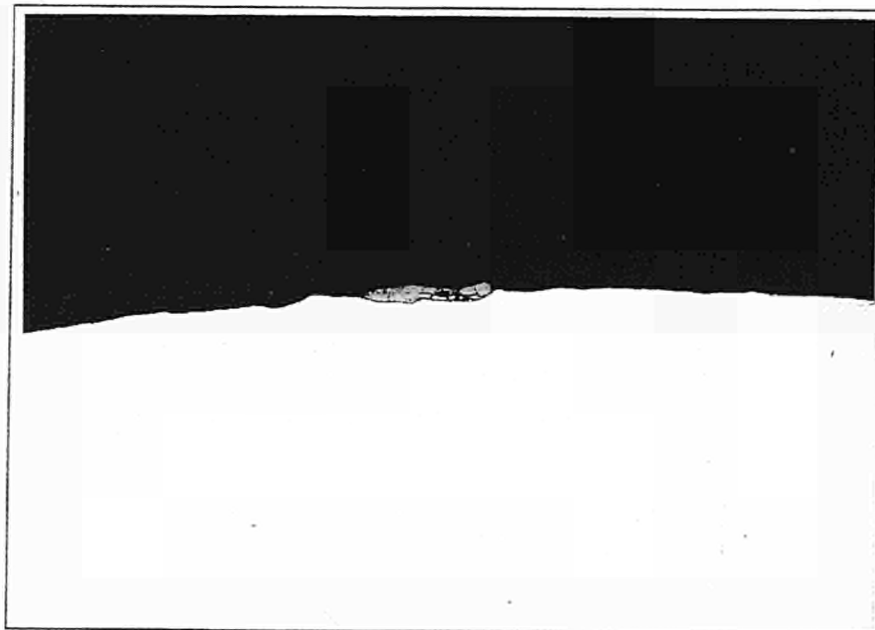
**FIG. 29**





Sample B

x 20



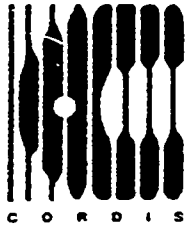
Sample C

x 20

**MACROPHOTOGRAPHS OF RESISTIVELY HEATED  
DEFECT SAMPLES**

**FIG. 30**





The Communities research and development  
information service  
**C O R D I S**

**A vital part of your programme's  
dissemination strategy**

CORDIS is the information service set up under the VALUE programme to give quick and easy access to information on European Community research programmes. It is available free-of-charge online via the European Commission host organization (ECHO), and now also on a newly released CD-ROM.

***CORDIS offers the European R&D community:***

- a comprehensive up-to-date view of EC R&TD activities, through a set of databases and related services,
- quick and easy access to information on EC research programmes and results,
- a continuously evolving Commission service tailored to the needs of the research community and industry,
- full user support, including documentation, training and the CORDIS help desk.

***The CORDIS Databases are:***

**R&TD-programmes – R&TD-projects – R&TD-partners – R&TD-results  
R&TD-publications – R&TD-comdocuments – R&TD-acronyms – R&TD-news**

***Make sure your programme gains the maximum benefit from CORDIS***

- Inform the CORDIS unit of your programme initiatives,
- contribute information regularly to CORDIS databases such as R&TD-news, R&TD-publications and R&TD-programmes,
- use CORDIS databases, such as R&TD-partners, in the implementation of your programme,
- consult CORDIS for up-to-date information on other programmes relevant to your activities,
- inform your programme participants about CORDIS and the importance of their contribution to the service as well as the benefits which they will derive from it,
- contribute to the evolution of CORDIS by sending your comments on the service to the CORDIS Unit.

**For more information about contributing to CORDIS,  
contact the DG XIII CORDIS Unit**

*Brussels*  
Ms I. Vounakis  
Tel. +(32) 2 299 0464  
Fax +(32) 2 299 0467

*Luxembourg*  
M. B. Niessen  
Tel. +(352) 4301 33638  
Fax +(352) 4301 34989

To register for online access to CORDIS, contact:

ECHO Customer Service  
BP 2373  
L-1023 Luxembourg  
Tel. +(352) 3498 1240  
Fax +(352) 3498 1248

***If you are already an ECHO user, please mention your customer number.***



European Commission

**EUR 15814 — Measurement and analysis**  
**Surface inspection of hot bars during rolling**

*D. Savidge*

Luxembourg: Office for Official Publications of the European Communities

1996 — XVIII, 41 pp. — 21.0 x 29.7 cm

Technical steel research series

ISBN 92-827-7122-9

Price (excluding VAT) in Luxembourg: ECU 7

The traditional method of inspecting the surface of hot steel bars has been to use surrounding coil eddy-current techniques which have inherent deficiencies. These systems of inspection are insensitive to long seam defects and also transverse defects and are generally limited to bars which are less than 75 mm in diameter. The object of this ECSC project is to develop an alternative method that can overcome these deficiencies and extend the range of bar sizes that can be tested.

The development of water-cooled inspection probe assemblies which are capable of being grouped around the bar circumference and the development of very stable electronics for signal processing have been the key features associated with the success of this project.

Plant trials with a five channel inspection head confirmed the defect detection capability, and the excellent signal-to-noise ratios suggest that defect detection limits may well be improved down to the 0.5 mm level.

These developments indicate that an improved method of hot bar inspection is now entirely feasible which overcomes the major deficiencies of existing bar testing installations.





## NOTICE TO THE READER

All scientific and technical reports published by the European Commission are announced in the monthly periodical '**euro abstracts**'. For subscription (1 year: ECU 63) please write to the address below.

---

Price (excluding VAT) in Luxembourg: ECU 7

ISBN 92-827-7122-9



OFFICE FOR OFFICIAL PUBLICATIONS  
OF THE EUROPEAN COMMUNITIES

L-2985 Luxembourg



9 789282 771228 >